A FUNCTIONAL INVESTIGATION OF THE *DIP1* GENE

A FUNCTIONAL INVESTIGATION OF THE *DIP1* GENE IN *DROSOPHILA MELANOGASTER*

By

JENNIFER KINDER, B.Sc.

A Thesis

Submitted to the School of Graduate Studies

In Partial Fulfillment of the Requirements

For the Degree

Master of Science

McMaster University

MASTER OF SCIENCE (2005) McMaster University

(Biology) Hamilton, Ontario

TITLE: A Functional investigation of the *DIP1* gene in *Drosophila melanogaster*

AUTHOR: Jennifer Kinder, B.Sc. (McMaster University)

SUPERVISOR: Dr. Ana Campos

NUMBER OF PAGES: x, 98

ABSTRACT

Reported here is the isolation and molecular characterization of two novel alleles of the *DIP1* gene; GE89 and GE77. As well, a third deletion of the *DIP1* gene, EY*4, isolated by our collaborators in France was characterized. PCR and sequencing analysis confirms all three alleles to be molecular deletions of the *DIP1* gene. However, in none of these cases is the entire gene excised. Also, immunohistochemistry of ovaries from each of these strains does not demonstrate a complete lack of DIP1 protein expression in any of the deletion strains. Thus, it appears that some protein product is being formed in each case. However, it is not clear whether this protein is functional. An assay was also conducted to investigate a function for DIP1 in mechanisms of epigenetic gene silencing. Although the findings of these experiments are incomplete, it appears that DIP1 may play a functional role in heterochromatin formation and/or post-transcriptional gene silencing. Interestingly, appendage formation phenotypes were observed in the original P-element insertion line as well as a female sterility phenotype in the GE77 allele. Overall, *DIP1* is an interesting double stranded RNA binding protein. Newly isolated alleles of the *DIP1* gene will be useful tools for further investigation of the functional role of this gene.

ACKNOWLEDGEMENTS

I would like to thank all those people who believed in me throughout the course of my Masters degree: especially when I doubted myself. Firstly, thanks to Dr Ana Campos for inviting me into her lab and convincing me to stay on to do graduate work. Thank you also to Dorothy De Sousa who initiated me into the lab and taught me my first laboratory skills. I would also like to give a special thanks to the Campos girls. Maria, Nadia and Veronica thanks for your emotional supporting and sharing your knowledge. I can also not forget Xiao Li – especially her special vegetarian dumplings. Of course, a big thank you is owed to Jessica Jackson. Her hard work contributed a lot to the completion of this document. Last but not least I must thank my mom Julie, my dad Dave and my brother James without whom I would never have been able to complete this project. Their unconditional support was invaluable to me.

TABLE OF CONTENTS

LIST OF FIGURES

LIST OF TABLES

LIST OF ABBREVIATIONS

ATG – Transcription start site

BDGP – Berkeley Drosophila Genome Project

DIP1 – Disco interacting protein 1

dsRBD – double stranded RNA binding domain

dsRBP – double stranded RNA binding protein

H3K9Me – Histone 3 Lysine 9 Methylation

HP1 – Heterochromatin Protein 1

miRNA – micro RNA

NLS – Nuclear Localization Signal

PEV – Position Effect Varriegation

PTGS – Post Transcriptional Gene Silencing

RISC – RNA-induced silencing complex

RITS – RNA-induced Initiator of Transcriptional Gene Silencing complex

siRNA – small interfering RNA

TGS – Transcriptional Gene Silencing

Chapter I

Introduction

***Disco Interacting Protein 1 (DIP1)* is a novel double stranded RNA Binding Protein (dsRBP).**

Disco Interacting Protein 1 (DIP1) was identified due to its interaction with the N-terminus of the *Drosophila melanogaster* protein disconnected (disco) in a modified yeast two-hybrid interaction screen (DeSousa et al., 2003). Disco is a zinc finger protein required for proper formation of the connection between the larval optic nerve and its target brain cells (Steller et al., 1987, Campos et al., 1995). Following identification of DIP1 as a putative regulator of disco an effort was made to characterize the *DIP1* gene and investigate its interaction with disco. This investigation pointed towards *DIP1* as a gene of interest in its own right with possible implications for future understanding of its interaction with *disco*.

The *DIP1* gene is encoded in the 20A region of the X-chromosome in close proximity to the centromere and an area of heterochromatin. Putative motifs contained within the DIP1 protein were identified by using bioinformatics techniques and the web tool BLAST (Pelka, 2000). Figure 1 (reproduced from (DeSousa et al., 2003, Pelka, 2000) depicts the features identified by this analysis, as well as, the genomic organization of the *DIP1* gene and three of the four confirmed DIP1 isoforms. Most interestingly, a putative nuclear localization signal (NLS) spans exons 2 and 3. Also, two putative translation start sites (ATGs) were identified.

Two regions similar to double stranded RNA Binding Domains (dsRBDs) were also identified. Northwestern analysis of the DIP1c isoform demonstrated that the dsRBDs preferentially bind double stranded RNA homopolymers and structured RNAs as opposed to single stranded RNA (Pelka, 2000). Thus, DIP1 has been classified as a double stranded RNA binding protein (dsRBP).

Four DIP1 isoforms were identified by northern blot of 0-16 hour embryonic mRNA (Bondos et al., 2004). cDNAs corresponding to three of these isoforms had previously been identified (Pelka, 2000). Variability among isoforms is accounted for by differential splicing between the first and second exons (Figure 1). The fourth isoform (not shown), annotated as DIP1d, splices out exon 2 completely thus removing the putative nuclear

localization signal. As well, inclusion of a variable number of repeats in the 3' untranslated region contributes to the complexity of this gene and is strain specific.

DIP1 protein expression is ubiquitous throughout development.

Investigation of the developmental expression pattern of DIP1 using a polyclonal anti-DIP1 antibody reveals widespread expression of DIP1 protein (DeSousa et al., 2003). In embryonic tissues, as well as adult ovaries and third instar larvae imaginal discs DIP1 protein localization appears to be predominantly nuclear (DeSousa et al., 2003). This observation is consistent with the finding of a putative NLS encoded within the *DIP1* gene. As well, DIP1 expression is apparent in the ring canal structures of adult ovaries connecting the nurse cells to the developing oocyte (DeSousa et al., 2003). This demonstrates non-nuclear localization of the DIP1 protein and correlates with the findings of Bondos et al. (2004) who isolated the DIP1d isoform in which the putative NLS is spliced out.

The pattern of DIP1 protein expression also appears to be associated with regions of active transcription (DeSousa et al., 2003). Firstly, in embryos, localization of DIP1 to the nucleus corresponds with the onset of zygotic transcription (DeSousa et al., 2003). Also, a different pattern of DIP1 expression is observed in embryonic mitotic domains suggesting reduced DIP1 protein at this site of lowered transcriptional activity (DeSousa et al., 2003). DIP1 has also been shown to associate with the interband and heat shock puff regions of polytene chromosomes which are known regions of active transcription (unpublished data, De Sousa). Another group of researchers also found DIP1 to bind to distinct chromosomal bands (Krauss et al., 2000, Krauss et al., 2001). This evidence supports a role for DIP1 in the control of gene expression.

Overexpression of DIP1 results in cell fate transformations

To facilitate further investigation of the function of DIP1, the expression pattern of DIP1 was manipulated using the UAS-GAL4 system. Generally, ubiquitous overexpression of DIP1 during embryogenesis results in organism lethality (DeSousa et al., 2003). However, tissue specific DIP1 overexpression typically results in cell fate transformations (DeSousa et al., 2003). Using the *eyeless* GAL4 driver overexpression of

DIP1 caused approximately 80% lethality (DeSousa et al., 2003). Interestingly, duplications, deletions and the formation of ectopic structures were observed in those flies that survived to the adult stage (DeSousa et al., 2003). Subsequently, investigation of gene expression in third instar larva imaginal discs, following overexpression of DIP1, revealed altered expression of genes involved in specification of head structures (DeSousa et al., 2003). These transformations were observed in tissues in which *eyeless* was no longer driving DIP1 expression. Hence, the altered phenotypes resulted from a pulse of DIP1 expression in early first instar, the effects of which were maintained for subsequent rounds of mitotic cell division.

Characterization of the *DIP1* gene appears to suggest a functional role for DIP1 in control of gene expression. A specific instructive role in development looks to be excluded due to the observed ubiquitous DIP1 expression pattern and range of phenotypes that occurred upon overexpression of DIP1. However, a pulse of DIP1 overexpression during embryogenesis and early first instar was sufficient to establish and maintain alterations in gene expression. Thus, further investigation may reveal a role for DIP1 in epigenetic maintenance or suppression of gene expression.

P-element mutagenesis is a useful approach for reverse genetics analysis of gene function.

To date the expression pattern and molecular organization of the *DIP1* gene have been well characterized. Additional investigation of the *DIP1* gene has been focused on the generation of mutant alleles. P-element transposition is one of the most useful tools for a reverse genetics approach to analysis of gene function. It has been predicted that P-element mediated mutations will be helpful in the characterization of more that 85% of the genes encoded in the *Drosophila melanogaster* genome (Spradling et al., 1999). Currently, the Berkeley Drosophila Genome Project (BDGP) gene disruption collection contains 7140 unique P-element insertion stocks (Bellen et al., 2004). All of these lines are available from the Bloomington Stock Center (http://flystocks.bio.indiana.edu/). A Korean based company, GenExel, also maintains a database of EP-element insertions that can be accessed via http://genexel.com/eng/htm/genisys.htm. Overall, P-element

mutagenesis has been shown to be an effective way to direct mutation of a specific gene. This approach has also been useful for the investigation of the *DIP1* gene.

dsRNA Binding Proteins (dsRBP) have been shown to be involved in a variety of functions including Post Transcriptional Gene Silencing.

The number of dsRBPs being identified is growing, and with that the number of different roles played by these proteins is also increasing. Among other functions, dsRBPs have been implicated in cellular functions from RNA localization to RNA editing and the host viral response (Saunders and Barber, 2003). In addition, dsRBPs have also been found to contribute to post transcriptional gene silencing (PTGS) (Doyle and Jantsch, 2002). Most notably, the RNase III enzyme Dicer (Dcr1 and Dcr2) was identified as the dsRNA binding enzyme that digests dsRNA into siRNA to initiate the RNAi pathway in *Drosophila* (Bernstein et al., 2001), mouse (Nicholson and Nicholson, 2002) and *C. elegans* (Knight and Bass, 2001). A clearer understanding of the role fulfilled by dsRBPs will be obtained as additional members of this diverse group of proteins are identified and characterized.

dsRBPs are defined by the inclusion of one or more regions of amino acid (aa) sequence similar to a 65-68aa consensus sequence (St Johnston et al., 1992). Two types of dsRBDs have been defined. Domains with strong homology to the entire length of the consensus sequence are termed Type A, while those with homology only to the C-terminal region of the consensus sequence are termed type B (Doyle and Jantsch, 2002). It should be noted that the *DIP1* gene encodes two dsRBDs; the first (dsRBD1) is of type A while dsRBD2 is of type B (DeSousa et al., 2003,Pelka, 2000).

Investigation of the class of proteins encoding dsRBDs has revealed a growing group of proteins involved in a wide range of cellular functions. Identification of DIP1 as a dsRBP, as well as its initial characterization, has interesting implications for a role for DIP1 in regulation of gene expression. Recent identification of dsRBPs with a role in PTGS suggests that it may also be worth while to look for a role for DIP1 in this mode of regulation of gene expression.

Post Transcriptional Gene Silencing and the RNAi pathway.

While heterochromatin formation effectively silences gene expression at the level of transcription, mechanisms also exist in the cell for post-transcriptional gene silencing (PTGS). The RNAi pathyway, in which a dsRNA molecule is recognized and triggers degradation of itself and homologous nascent transcripts, prevents translation of specific mRNA templates (Hannon, 2002). Effectively, through the RNAi pathway gene expression is silenced at the post-transcriptional level.

To date several of the key players in RNAi mediated gene silencing have been characterized. Firstly, Dicers are a family of ATPase/RNA helicase proteins which encode two catalytic RNase III domains and a C-terminal dsRNA binding domain (Bernstein et al., 2001). The primary role of these proteins is to initiate RNAi by chopping up precursor RNA into siRNA or miRNA (Filipowicz, 2005). siRNA molecules are incorporated into the RNA-induced silencing complex (RISC) (Hannon, 2002). One protein family found consistently in the RISC complex is the Argonaute family which can be subdivided into two groups, Ago and Piwi, both of which are characterized by PAZ and PIWI domains (Filipowicz, 2005). Additional components of the RISC complex may include small dsRBPs and proteins with RNA helicase/ATPase domains (Filipowicz, 2005). However, it has been shown that a functional recombinant RISC can be formed by combination of human Argonaute2 with a siRNA molecule (Rivas et al., 2005). All of the components of the RNAi pathway contribute to the efficient recognition of precursor dsRNA, subsequent enzymatic breakdown of the RNA into siRNA molecules and targeted silencing of specific similar sequences.

Heterochromatin formation silences gene expression at the level of transcription.

Our current understanding of the *DIP1* gene suggests that DIP1 plays a role in epigenetic regulation of gene expression. It has been shown that heritable modifications of chromatin structure are one way in which gene expression is statically maintained in an active or a suppressed state. Chromatin can take on two basic forms: heterochromatin or euchromatin (Grewal and Moazed, 2003). Heterochromatin is typically described as condensed chromatin and is visible in *Drosophila* polytene chromosomes as regions of

dense staining. Generally, heterochromatin is inaccessible to transcription factors and is protected from extensive nuclease digestion (reviewed in Dillon, 2004). Packaging of DNA into heterochromatin also limits gene expression (Elgin and Grewal, 2003). Given that the *DIP1* gene has been proposed to be involved in epigenetic regulation of gene expression and that heterochromatin formation is one method of transcriptional gene silencing, it may be interesting to look at possible interactions between DIP1 and heterochromatin formation or stabilization. Firstly, a more complete review of the properties of heterochromatin is necessary.

Heterochromatin is defined as regions of chromatin which remain condensed throughout the cell cycle (Richards and Elgin, 2002). Two types of heterochromatin have been described. Firstly, constitutive heterochromatin encompasses all forms of heterochromatin that are found globally in all cells, such as telomeric and centromeric heterochromatin as well as the heterochromatization of repetitive sequences. Alternatively, facultative heterochromatin describes cell specific and clonally inherited silencing of specific regions of the genome (Elgin and Grewal, 2003). The characteristics and formation of facultative heterochromatin are of most interest to understanding regulation of gene expression.

Biochemically, heterochromatin can be recognized by several hallmarks. Firstly, areas of heterochromatin are characterized by hypo-acteylation of histones 3 and 4 (Nakayama et al., 2001). Methylation of histone 3 lysine 9 (H3K9Me) is also observed in these areas (Elgin and Grewal, 2003). Finally, methylation of DNA cytosine residues has also been associated with heterochromatin in plants and mammals (Elgin and Grewal, 2003, Mathieu and Bender, 2004). However, it should be noted that DNA does not appear to be methylated in *Drosophila melanogaster* (Henikoff and Matzke, 1997). The characteristic marks of heterochromatin listed here indicate the alterations that mediated the DNA conformational change from chromatin to heterochromatin.

The procedure of forming heterochromatin is an involved and complex process however, for the purposes of this overview several general steps should be mentioned. Methylation of H3K9 is mediated by a histone methyl transferase enzyme known as

Su(var)3-9 in *Drosophila,* Clr4 in fission yeast and SUV39H1 in humans. However, methylation of this residue cannot occur without previous deacetylation. Deacetylation of H3K9 is mediated by the Histone Deacetylase 1 (HDAC1) protein (Czermin et al., 2001). Following histone methylation, the Heterochromatin Protein 1 (HP1) protein (or Swi6 in fission yeast) is also recruited which binds to methylated H3K9 (Elgin and Grewal, 2003). Association of HP1 and Su(var)3-9 to chromatin has been shown to be interdependent (Schotta et al., 2002). It is also remarkable that both HDAC1 and HP1 have been shown to associate with Su(var)3-9 by immunoprecipitation of *Drosophila* embryonic extracts (Czermin et al., 2001,Schotta et al., 2002). Similar results were found in *S. pombe* in which methylation by Clr4 and association of Swi6 were dependent on proper functioning of the histone deacetylase Clr3 (reviewed in Grewal and Elgin, 2002).

Interestingly, an interaction between Su(var)3-9 and DIP1 has also been suggested by results from a yeast two-hybrid screen looking for interactors of Su(var)3-9 (Krauss et al., 2000,Krauss et al., 2001). This result suggests a possible functional role for DIP1 in regulating or maintaining heterochromatin formation and has directed our attention towards investigating DIP1 interactions with silencing paradigms.

Proposed mechanisms for epigenetic maintenance of heterochromatin include recognition of DNA methylation and histone modifications.

Inheritance of heterochromatin through generations of cell division has been indicated as a way in which epigenetic gene regulation is mediated. The biochemical marks of heterochromatin discussed above appear to be implicated in the process of recognition and perpetuation of gene silencing. One mechanism for heritable maintenance of heterochromatin involves recognition of DNA cytosine methylation (reviewed in Richards and Elgin, 2002). DNA methylation is maintained on the parental strand during DNA replication. Following DNA replication, specific cytosine methyl transferase enzymes recognize hemi-methylated DNA and catalyze restoration of the full methylation pattern. Thus, heterochromatization of specific areas of the genome is maintained through cell division.

However, a similar pattern of methylated cytosine molecules has not been indicated as a mark of heterochromatin in *Drosophila* and other lower eukaryotes (Henikoff and Matzke, 1997). In this case it has been suggested that modifications of the histones mediate cellular memory of heterochromatization (Grewal and Elgin, 2002). Parental histones have been shown to be reused efficiently in repackaging of replicated DNA and are assorted randomly to daughter DNA strands (reviewed in Richards and Elgin, 2002). Thus, parental modified histones remain associated with silenced areas of the DNA and enable recruitment of enzyme complexes to modify newly synthesized histones. In this manner, silencing of a specific area of the genome may be perpetuated through continuous rounds of cell division.

RNA directed transcriptional gene silencing by specifying heterochromatin formation.

Recently, a coupling of the RNAi pathway of PTGS with heterochromatin formation and transcriptional gene silencing (TGS) has been a subject of intense investigation. It is well known that heterochromatin formation leads to epigenetically maintained gene silencing. As well, the RNAi system has been shown to effectively eliminate translation of targeted RNA transcripts. However, it is not well understood how areas of the genome become targeted for heterochromatin formation and ultimately specified for gene silencing at the level of transcription. Currently, a large body of evidence suggests the RNAi system as a bridge to targeting regions of the genome for heterochromatin formation and thus transcriptional gene silencing.

A mechanism for RNA mediated heterochromatin formation has been proposed based on a large amount of evidence collected from experiments with *S. Pombe* (Grewal and Rice, 2004). This system is triggered in much the same way as the RNAi pathway. Firstly, dsRNA is transcribed from the genome. Often regions that will be targeted for gene silencing initiate bi-directional transcription, thus, pairing of the two transcribed strands will form dsRNA which is necessary for recognition by the RNAi pathyway (Allshire, 2002). Following recognition of the dsRNA by the Dicer enzyme dsRNA is cut up into pieces of RNA approximately 20bp in length termed siRNA (Verdel et al., 2004).

The presence of these small nucleic acid molecules initiates Ago binding and formation of the RNA-induced Initiator of Transcriptional gene silencing complex (RITS) (Verdel et al., 2004).

The RITS complex is similar to the RISC complex. Like RISC, the RITS complex contains an Ago protein. In addition, a chromodomain protein essential for H3K9 methylation is also a component of the RITS complex (Verdel et al., 2004). Also, the RITS complex becomes associated with sites in the genome complementary to the associated siRNA. Association of the RITS complex with genomic DNA initiates H3K9 methylation. Recall, methylated lysine 9 on histone 3 is a biochemical hallmark of heterochromatin. Amplification of the silencing signal induced by the RITS complex is mediated by association with another complex termed the RNA-directed RNA polymerase (RDRP) complex (Motamedi et al., 2004). The components of this complex are responsible for the production of secondary RNA transcripts from the silenced region thus maintaining the source of dsRNA necessary for the maintenance of silencing. In this way dsRNA, via the RNAi pathway, appears to direct heterochromatin formation at specific genomic sites.

Position effect variegation

To date, a large amount of data has been collected regarding mechanisms of epigenetic gene regulation. However, our understanding of this process is far from complete. A classical method that has been used extensively, and continues to be valuable, for the identification of modifiers of heterochromatin formation and/or stabilization is Position Effect Variegation (PEV). Position effect variegation is defined as the variegated expression of a gene in the cells where it is normally expressed due to its relocation (by transposition or chromosomal inversion) near a region of heterochromatin (Elgin and Grewal, 2003). This variegating pattern of expression is due to 'spreading' or an expansion of neighbouring heterochromatic silencing. As discussed above, heterochromatic silencing is set up by methylation of H3K9 and recruitment of the HP1 protein. Establishment of these characteristics has been postulated to be able to affect adjacent areas of the genome (Grewal and Moazed, 2003). Thus, localization of a

gene adjacent to an area of heterochromatin will sometimes result in silencing of the expression of that gene.

The PEV phenomenon is a very useful tool for identifying functional components maintaining epigenetic gene regulation. One PEV rearrangement that has been shown to be particularly useful is the $In(1)w^{m4}$. In this strain, the *white* gene encoded on the X-chromosome has been inverted into close proximity to a region of constitutive heterochromatin (Schotta et al., 2003). This line has variegated eye pigment. Addition of a suppressor of variegation will increase the amount of eye pigment produced. Conversely, the addition of an enhancer of variegation will further reduce the amount of eye pigment produced. In this way, mutant alleles altering heterochromatin formation and/or stabilization can be visually detected. This system (and other similar PEV rearrangements) has been used successfully to identify over 50 modifiers of PEV (Grewal and Elgin, 2002). One specific example is the identification of Su(var)3-9 as a suppressor of PEV. Further use of this straight forward assay is likely to identify further components of the epigenetic regulation of gene expression system. It is also possible that an interaction with PEV may be found with mutant alleles of the *DIP1* gene.

Repeat induced gene silencing

Another phenomenon which results in variegated gene expression is known as repeat induced gene silencing (or RIGS especially in plants). It has been shown that tandem or inverted repeats of DNA ultimately lead to their own silenced expression due to heterochromatin formation (Dorer and Henikoff, 1997,Dorer and Henikoff, 1994). Silencing of repeat regions usually occurs in a variegated pattern with the strength of variegation dependent on the number of repeats present (Dorer and Henikoff, 1994). Overall, a larger number of repeats results in increased silencing. As well, inverted repeats show stronger variegation compared to similar tandem repeats (Dorer and Henikoff, 1994). Although repeats found in areas close to heterochromatin show a stronger effect, silencing of the DNA array is not dependent on its position in the genome (Dorer and Henikoff, 1994). Of most interest is the finding that genetic modifiers of PEV also modify repeat induced gene silencing (Dorer and Henikoff, 1994). As well, array

silencing can also affect the expression pattern of neighbouring genes (Dorer and Henikoff, 1997). Taken together these observations support the hypothesis that array silencing is due to localized heterochromatin formation.

More recently, the repeat induced gene silencing phenomenon in *Drosophila* was used to link mutations of the RNAi pathway to heterochromatin formation (Pal-Bhadra et al., 2004). In their experiments Pal-Bhadra and colleagues (2004) looked at the effects of mutations of the *piwi* and *homeless* genes, known to play a role in the RNAi pathway, on *mini-white* expression in several strains carrying *mini-white* arrays. Decreased silencing, or increased eye pigment expression, was observed with both mutations indicating heterochromatin was not properly formed in either of these cases. Therefore, it appears that proper functioning of the RNAi pathway is necessary for establishment of silencing at repeated loci in the *Drosophila melanogaster* genome. This provides evidence for the hypothesis that siRNA plays a role in targeting homologous DNA for silencing via heterochromatin formation.

DIP1 mutagenesis and functional investigation.

The goal of this thesis project is to isolate deletions of the *DIP1* gene by P-element mutagenesis and to investigate possible functional roles for this gene in *Drosophila melanogaster*. A role for this novel dsRBP in epigenetic regulation of gene expression has been proposed. Techniques used to identify components of the RNAi pathway and heterochromatic gene silencing pathway will be used to further investigate a role for *DIP1* in epigenetic regulation of gene silencing.

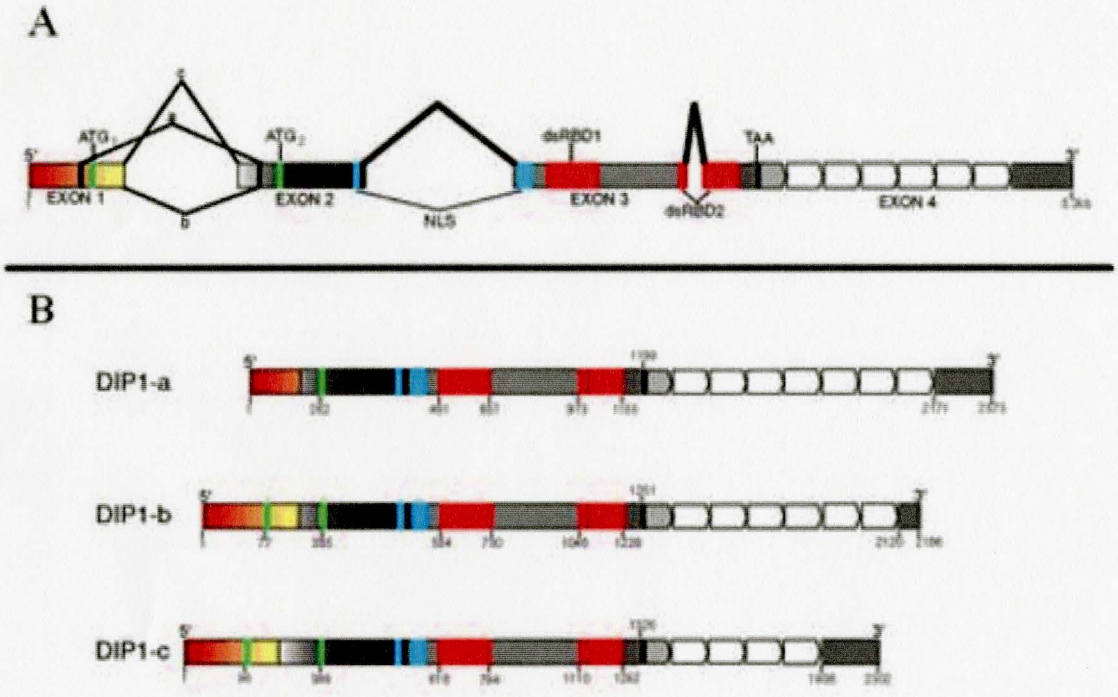

Figure I : Genomic organization of DIP1 gene

(Reproduced from De Sousa et al., 2003, and Pelka, 2000 Master Thesis

Chapter II

Materials and Methods

Fly Strains

P-element stocks used for the experiments described here include BG2658 (Bloomington 13912), EY2625 (Bloomington 15577) and GE50031 (now known as GenExel G1261). FM7j was used as a homozygous viable X-chromosome balancer (Bloomington 6417) marked with bar eyes (B^1). $Dp(1;Y)y^+mal^{106}$ is a duplication of the X-chromosome on the Y-chromosome that was used to balance deletions of the X-chromosome. A number of deficiency lines were used which carry a deletion that spans the *DIP1* region of the X-chromosome. Df(1)LB6 (Bloomington 5999) has cytologically defined breakpoints 19E2-20A3 while Df(1)exel 6255 has well defined breakpoints 20A1-20B1 (Bloomington 7723). Additional deficiency lines with breakpoints proximal to *DIP1* were also used. Df(1)R21 (Bloomington 5972) has cytological breakpoints 20A2-20A3 while Df(1)R38 (Bloomington 6308) has cytological breakpoints 20A2-20A4; 20E1-h26. Mini-white array lines were obtained from the Henikoff lab (Howard Hughes Medical Institute). w^{1118};P[lacWx2]1A6/CyO is a tandem duplication of P[lacW]. w^{1118};P[lacWx6]BX1/CyO and w^{1118};P[lacWx6]DX1/CyO both have 6 copies of P[lacW] 1 of which is inverted. w^{1118};P[lacWx3]FX1/CyO has 3 copies of P[lacW] the middle one is inverted. Lines 1A6 and FX1 were found to be homozygous non-viable. Lines BX1 and DX1 are viable, but non fertile, as homozygotes. The X-chromosome inversion stocks used for PEV experiments are available from Bloomington: $In(1)w^{m4}$;Su(var)3-9^1/TM3,Sb^1,Ser^1 (Bloomington 6209) and $In(1)w^{m4}$;Su(var)3-9^2/TM3,Sb^1,Ser^1 (Bloomington 6210).

Ni-NTA affinity purification of His-tagged protein

See Peter Pelka Masters Thesis 2000.

Protein Purification by Gel Electro-elution

A single colony of DIP1a in pET21b+ BL21(DE3) was used to inoculate 5ml of SOB plus Kanamycin and grown overnight at 37°C with vigorous shaking. The following morning the 5ml starter culture was diluted to 1:50 in 250ml SOB plus Kanamycin in a 2L flask. Bacterial growth was stimulated by vigorous shaking at 37°C until an OD_{600} reading of 0.6 was obtained (approximately 2-2.5 hours). Once an OD_{600} of 0.6 was

reached, IPTG was added to a final concentration of 1mM. Protein production was induced by continuing to shake the media at 37°C for another 4.5 hours. Following induction, cells were harvested by centrifugation at 4 000 x g for 20 minutes. The supernatant was then removed, leaving as little liquid behind as possible, and the cell pellet was stored at -20°C overnight. In order to obtain cleared cellular lysate from the cell pellet the pellet was first washed with a small amount of PBS and re-spun at 4 000 x g for 20 minutes at 4°C. The washed pellet was then resuspended in an 8M Urea pH 8.0 denaturing solution at a volume of 5ml per gram of pellet. Lysis was completed by gentle stirring until the entire pellet was dissolved and the solution became translucent (approximately 30-45 minutes). Cellular debris was removed by centrifugation at 10 000 x g for 30 minutes. Cleared lysate can be run directly on an SDS-PAGE gel. In this case, 500µl of cleared lysate was run on a large 12% SDS-PAGE gel at 100 to 200 Volts until the loading buffer reached the bottom edge of the gel. The gel was then removed from the apparatus and a strip cut off one or both edges. These strips were stained with Coomassie stain for at least 15 minutes while the remainder of the gel was wrapped in plastic wrap and kept at 4°C. Stained strips were then destained for approximately 1 hour, with frequent changing of the destaining solution, until the target protein location was visualized. Following destaining, the cut off strips were realigned with the remainder of the gel enabling the portion of the unstained gel corresponding to the target protein to be excised. For accuracy, after excising the target protein the remainder of the gel was stained. Next, the target protein strip was cut into small pieces and placed in a dialysis tubing bag with approximately 2ml Electro-elution Buffer (25mM Tris, 192mM Glycine, 0.1% SDS). Often, the target protein strip and Electro-elution Buffer were split between two smaller dialysis tubes. In the final step, the dialysis tubing was placed crosswise in a horizontal gel box filled with Electro-elution Buffer and run at 10-15 Volts for approximately 16 hours at 4°C. At the end of the run, the current direction was reversed for 30 minutes in order to dislodge any protein that had stuck on the dialysis tubing. Finally, eluted protein was removed from the dialysis tubing and dialyzed overnight

against 1X PBS at 4°C. The concentration and purity of Electro-eluted protein was assessed by SDS-PAGE gel and comparison to BSA protein standards.

Affinity Purification of Antibodies using Antigen Immobilized on Nitrocellulose Filters (adapted from Pelka Master's Thesis, 2000 and Molecular Cloning: A laboratory Manual 2nd Ed. Sambrook *et al.*, 1989)

Approximately 500µg of purified recombinant DIP1a protein was loaded along the entire length of a small 12% SDS-polyacrylamide gel and run at 200V until the loading buffer traveled to the bottom edge of the gel. The protein was transferred to a PVDF membrane in a transfer apparatus run at 60V for 3 hours at 4°C. Following transfer, the membrane was stained with fresh Ponceau S solution (Sigma) for 20 minutes at room temperature. The membrane was then washed with water until the DIP1a protein band was visible. The thin strip of membrane corresponding to DIP1a recombinant protein was cut out and blocked for 1 hour in 10ml blocking buffer (3% BSA in 1 x PBS) at room temperature. The blocking buffer was then replaced with 4.5ml fresh blocking buffer plus 500µl rabbit sera produced by Pocono Rabbit Farm. The membrane was incubated in the antibody solution for approximately 16 hours on a rotary shaker at 4°C. The following morning the antibody solution was removed and the membrane was washed in 0.15M NaCl for 20 minutes followed by a rinse in 1 x PBS for an additional 20 minutes. The membrane strip was then arranged on a piece of Parafilm pressed into the bottom of a Petri dish and approximately 200-500µl of elution buffer (0.2M glycine (pH 2.8); 1mM EGTA) was pipeted onto it. The elution buffer was incubated on the membrane strip for 20 minutes in a humidified atmosphere at room temperature with gentle rocking. The eluted antibody was then transferred to an Eppendorf tube and neutralized by adding 0.1 volumes of 1M Tris-Cl pH 7.4. The pH was checked for near neutrality by spotting an aliquot on pH paper. Additional additions of Tris were made if necessary. Finally, 0.1 volumes of 10 x PBS were added and the antibody solution was dialyzed against 1 x PBS overnight. The purified antibody was stored at 4°C and was typically good for 3-6 months.

Immunohistochemistry of *Drosophila melanogaster* ovaries (similar to that described by De Sousa *et al.*, 2003)

The ovaries of 2-3 day old females were dissected in cold PBS and fixed in 4% paraformaldehyde in PBS for 20 minutes at room temperature. Following fixation, the ovaries were rinsed several times in PBT (1 x PBS with 0.2%TritonX) and then washed three times for five minutes to remove the fixative. The tissues were then blocked in a 1:15 solution of NGS:PBT (0.2%) for 1 hour. Purified primary anti-DIP1 antibody was then added at a concentration of 1:15 and incubated overnight at 4°C. The next day the antibody solution was removed and the ovaries were washed with PBT (0.2%) for 2-4 hours changing the solution every 30 minutes. Prior to addition of the secondary antibody the tissues were again blocked for 1 hour in a 1:15 solution of NGS:PBT (0.2%). Alexa 488 goat anti-rabbit secondary antibody was then added in a concentration of 1:200 and incubated overnight at 4°C. The secondary antibody was washed out for approximately 4-8 hours. The ovaries were mounted in 70% glycerol.

Single-fly DNA Prep for PCR (adapted from Gloor et al., 1993)

A single fly was collected and placed in an Eppendorff tube. A pipette tip containing 50µl of Squishing buffer (10mM Tris-Cl pH 8.2, 1mM EDTA pH 8.0, 25mM NaCl, 20µg/ml Proteinase K) was used to mash up the fly. The remaining Squishing buffer was then expelled and the solution incubated at 30-37°C for 30 minutes. Finally, to inactivate the Proteinase K the tube was heated to 95°C. Single-fly DNA preps were stored at 4°C for approximately 1-3 months. From these preps 5µl of DNA was used per 50µl PCR reaction.

Eye Pigment Extraction and Quantification (modified from Pal Bhadra et al., 2004 by Jessica Jackson)

15 flies of the desired phenotype were collected and allowed to age for 3 full days. The flies were then frozen at -80°C until use. The first step of the extraction process was to place the 15 flies in a screw cap tube and immerse it in liquid nitrogen. Subsequent shaking of the frozen tube served to decapitate the flies. The fly heads were sorted from the rest of the body parts and emulsified with 500ul 0.1% HCl in methanol (for 10ml of

solution mix 9.7ml methanol with 30ul 36%HCl). The mixture was then centrifuged at 15 000 rpm for 1 minute and an OD 480 measurement of the absorbance of the supernatant was carried out.

PCR and Sequencing

5µl of single fly DNA prep was sufficient for efficient PCR amplification of a DNA fragment. The primers used are described in the appendix. Standard program used: 94°C – 2min; (94 °C – 1min, 55 °C – 1min, 72 °C – 2min) 35X; 72 °C – 2min, 4 °C - ∞. Purification of PCR amplified DNA products for sequencing was done by agarose gel purification using a gel purification kit produced by Qiagen. Firstly, PCR product was run on a 0.8% agarose gel. A clean scalpel was used to excise the band from the gel removing as much excess agarose gel as possible. The gel slice was incubated with Buffer QG (300µl buffer/100mg gel) at 50°C for 10 minutes. The dissolved gel solution was then applied to the provided centrifuge column. Binding of the DNA to the column was mediated by centrifugation at 13 000rpm for one minute (repeated until all of the gel solution had passed through the column). Additional Buffer QG was applied to the column in order to remove all traces of agarose. 750µl of Buffer PE (with ethanol) was placed on the column to remove contaminating salts. DNA was eluted with 20µl sterile ddH_2O. To increase the yield the ddH_2O was incubated on the column for 10 minutes prior to centrifugation at 13 000rpm for 1 minute to elute the DNA. PCR product purified in this way was stored at -20°C and is suitable for subsequent sequencing reactions. Sequencing of purified PCR products was done by MobixLab located in the Life Sciences Building at McMaster University.

Sterility Assay

In order to determine the fertility phenotype of a particular fly strain, 20 female flies were individually crossed to two balancer male flies (usually FM7j/Dp(1:Y)) and kept at 25°C. After 20 days the number of progeny produced was counted.

Chapter III

Results

Purification of DIP1 Protein and anti-DIP1 antibody

A high quality specific antibody is an essential tool for the investigation of gene expression and gene function in *Drosophila melanogaster.* Previous characterization of the DIP1 protein expression pattern made extensive use of a DIP1 specific polyclonal antibody generated by our lab (Pelka, Masters Thesis, 2000, De Sousa *et al.*, 2003). Purified anti-DIP1 antibody can be extracted from whole sera using purified recombinant DIP1 protein.

Ni-NTA affinity purification of His-tagged DIP1 protein was unsuccessful.

To begin with, a purified source of recombinant DIP1a His-tagged protein was needed. Initially, purification was attempted by a Ni-NTA affinity column procedure (Qiagen) as had been done previously (Pelka, Masters Thesis, 2000). In this method the first step was to induce expression of the recombinant His tagged-DIP1 protein in bacteria. Figure 2A shows the time course of induction. A distinct band of induced DIP1 protein expression became visible at approximately 2 hours. The amount of DIP1 protein produced continued to increase with time maximizing at approximately 4.5 hours. At that time point the bacteria cells were harvested and lysed to release the contained proteins by solubilization in 8M Urea pH8.

Centrifugation was used to clear the lysate of cellular debris. A small sample of lysate was retained for SDS-PAGE gel analysis (Figure 2B & 2C induced ctrl). The remaining cleared lysate was then incubated with the Ni-NTA beads to bind His-tagged DIP1. These beads were used to construct a column and the liquid flow through was collected. SDS-PAGE gel analysis of the flow through (FT) is shown in Figure 2B and 2C. Comparison of the flow through to the unbound induced control does not show much of a difference in their compositions perhaps indicating inefficient binding of the His-tagged DIP1 recombinant protein with the column. Subsequently, washes with 8M Urea pH6.5 and pH6.25 were used to remove contaminants from the column (Figure 2B). In this case, there also appeared to be a significant loss of the target protein. Several other washes at lower pH were also carried out (not shown). Finally, at pH4.0 relatively pure DIP1 protein was eluted (Figure 2C). However, the yield of purified protein was

extremely low and unsuitable for further use. Thus, an alternative method for protein purification was sought out.

Gel electro-elution isolated a relatively large quantity of purified DIP1 protein.

One possible alternative method for protein purification is gel electro-elution. In this procedure, proteins are simply separated on an SDS-PAGE gel, the target protein is identified and excised and subsequently eluted. More specifically, in a similar manner to that described for the affinity column purification above, expression of the His tagged-DIP1 protein was induced in bacteria and the cells were lysed to release the contained proteins. However, instead of binding the lysate with the Ni-NTA beads the cleared lysate was run on an SDS-PAGE gel (Figure 3A, lane CL). Next, the band corresponding to DIP1 was cut out of the gel and an electrical current was applied to elute the protein.

From this protocol a fairly concentrated solution of purified DIP1a protein was obtained (Figure 3A, lane E). Coomassie gel comparison of the purified DIP1a protein with a BSA standard demonstrated an average yield of approximately 0.5mg DIP1a protein/mL electro-elution buffer. The purified protein was detected in a Western Blot by anti-DIP1 antibody and by anti-His antibody (Figure 3B). This protein was also suitable for use in further applications.

DIP1 protein purified by gel electro-elution was used to purify anti-DIP1 antibody.

Polyclonal anti-DIP1 antibody was purified by affinity binding with purified DIP1a recombinant protein immobilized on a PVDF membrane. In the first step of this procedure, purified DIP1 recombinant protein was loaded along the entire length of an SDS-polyacrylamide gel. The gel was then run at 200V until the loading buffer reached the edge of the gel. Next, the proteins in the gel were transferred to a PVDF membrane in a procedure equivalent to that of a Western blot. Following transfer, the entire PVDF membrane was subjected to Ponceau S staining. Ponceau S transiently binds to proteins enabling visualization of the proteins immobilized on the PVDF membrane without compromising them. Thus, the strip of membrane corresponding to DIP1 protein was identified and cut out. This strip was then incubated with whole sera facilitating binding of the DIP1 specific antibodies to the protein immobilized on the strip. Following

washing off of all materials not bound to the membrane, the purified antibody was eluted. Prior to use, the purified anti-DIP1 antibody was dialyzed against 1 x PBS overnight.

Immunohistochemistry of ovaries was used to test the specificity and concentration of the purified anti-DIP1 antibody. Antibody staining of wild type (OR) ovaries was done at concentrations of 1:10, 1:15 and 1:20 followed by examination of the ovaries by epi-fluorescence microscopy. The pattern of staining in all cases was very similar to that established previously (De Sousa *et al.*, 2003). It was determined that a concentration of 1:10 gave the best balance of distinct staining with an acceptable amount of background staining.

An attempt to generate a monoclonal anti-DIP1 antibody was unsuccessful.

An attempt was also made to generate a monoclonal antibody for DIP1. For this purpose, purified DIP1a recombinant protein was isolated by the electroelution procedure and shipped to Abnova Corporation in Taiwan. Prior to shipment, Amicon centrifuge tubes were used to change the buffering solution to 10mM Tris 1mM EDTA and concentrate the DIP1 protein solution to approximately 1mg/ml. The final protein concentration was checked by Commassie gel comparison to a BSA standard. Shipment of the purified DIP1 protein was done in liquid form and sent to Taiwan on solid CO_2. However, Abnova was unable to identify any anti-DIP1a positive clones.

Overall, a high concentration of purified DIP1 protein was isolated by the gel electroelution procedure. This protein was also used successfully to purify polyclonal anti-DIP1 antibody which was shown by immunohistochemistry of ovaries to specifically bind DIP1.

Disruption of *DIP1* gene expression by P-element mutagenesis generated novel potential *DIP1* alleles.

The construction of mutant *DIP1* alleles is an essential tool in the investigation of the function of the *DIP1* gene. One technique that has been successfully used to alter gene expression in *Drosophila melanogaster* is P-element mutagenesis. P-elements are pieces of DNA that in the presence of the enzyme transposase can undergo excision and/or insertion within the genome. The forms of excision and insertion include: precise

excision or removal of the P-element returning the DNA to its previous state, imprecise excision in which the P-element is removed along with a portion of the surrounding genome or mobilization in which the P-element is removed and subsequently re-inserted in a new location. P-element mobilization and imprecise excision were employed in this investigation in an attempt to generate insertions in and deletions of the *DIP1* gene.

P-element insertion lines in proximity to DIP1 facilitated DIP1 mutagenesis.

For the purposes of this study three different insertion lines (BG2658, EY2625 and GE50031) located in close proximity to the *DIP1* gene were obtained. The localization of each element is depicted in Figure 4B. The BG2625 insertion site is located 1354bp upstream of the 5' end of *DIP1*. The BG2625 element is a P{GT1} element which contains both a GAL4 and a white+ element (Bellen et al., 2004). As well, both the EY2625 and the GE50031 P-elements are inserted 23bp into the 5' UTR of *DIP1*. Although these two elements share an insert location, there are some significant differences between these two elements that should be noted. Firstly, the EY2625 element is derived from P{EPgy2}(Bellen et al., 2004) while the GE50031 P-element is an EP element constructed by Rørth (GenExel). Both of these elements carry a white+ gene as well as a GAGA/Gal4-UAS enhancer. However, the EY2625 element encodes a yellow+ marker in place of the kanamycin resistance found in the GE50031 element. As well, the orientation of these two elements is different such that the UAS motif in the GE50031 element when active would drive expression opposite to that of the *DIP1* gene (GenExel database).

A general genetic crossing scheme for inducing P-element mediated mutation of the *DIP1* gene is presented in Figure 5. In the P1 generation each P-element strain was crossed to an exogenous source of transposase (Δ2-3). Transposase in combination with the P-element enables mobilization of the transposable element. Single germline mobilization or excision events were recovered over an FM7 X-chromosome balancer and used to create broods carrying unique potential mutations. Single fly PCR was used to determine if a deletion had occurred. In those cases where a deletion was indicated, DNA sequencing was then used to determine the extent of the deletion.

A low rate of P-element excision was observed in the DIP1 region.

I have attempted to generate mutations in the *DIP1* gene using BG2658, EY2625 and GE50031 P-element insertion lines. One round of P-element mobilization was attempted using the BG2658 line as part of my undergraduate thesis. Another two rounds of excision and mobilization were undertaken with the EY2625 element. Finally, one large excision scheme was completed with the GE50031 insertion line. Overall, one line of interest (PE16) was generated from the BG2658 scheme. PE16 is a homozygous lethal line with a new P-element insertion site approximately 300bp 5' of the original BG2658 insertion site (see Figure 4B). No excision or mobilization lines of interest were generated by me in the EY2625 scheme. However, a parallel excision experiment conducted by our collaborators in France established a single deletion strain (EY*4) (Maryvonne Mével-Ninio, personal communication). My final attempt at establishing a DIP1 mutant using the GE50031 insertion line yielded 100 potential excision lines two of which were established as different deletion strains (see PCR and sequencing analysis below).

The observed rate of P-element excision for each mutagenesis scheme is reported in Table 1. In the BG2658 scheme 1374 individual flies were screened. Only those flies that were derived from the germline of flies exposed to transposase and that also lacked the active transposase element were included in this count. Of those observed, 24 were identified as potential mobilizations as detected by increased intensity of orange eye colour. Further analysis of these 24 lines identified 5 as homozygous sterile and 1 as homozygous lethal (results from Jen Kinder 4C09 thesis, 2003). 857 additional chromosomes that had been exposed to transposase were screened in the EY2625 scheme. Of those screened, 24 lines were identified as potential excisions based on lack of pigment expression in the eye. The final P-element excision scheme conducted in this study generated 100 potential excisions as identified by lack of mottled orange eyes. Overall, the rate of excision/mobilization in the *DIP1* region of the genome is approximately 2%-3% (Table 1).

In summary, mutagenesis of the *DIP1* gene was attempted in four different rounds of P-element mobilization or excision utilizing the three different P-element insertion lines. A low rate of excision/mobilization of approximately 2%-3% was observed. The potential excision lines identified require further analysis to identify any disruptions of the *DIP1* gene at either the molecular or the phenotypic level.

Three deletions of the *DIP1* gene were molecularly characterized by PCR and sequencing analysis.

Analysis of all potential excisions obtained in the EY2625 & GE50031 P-element mutation schemes was conducted by PCR. Figure 4B depicts the location of the primers used in this analysis. Further details about each primer are available in the appendix.

An initial PCR scan for both upstream and downstream deletions of the DIP1 gene identified two novel lines for further investigation.

Two sets of primers were used in an initial scan of each unique potential excision line. The first set, ML11486 and ML11487, were designed to amplify a 500bp region directly 5' of the EY2625 or GE50031 insertion site. As well, primers AB28564 and ML1750 were used to amplify a 1.8Kb region immediately 3' of the EY2625/GE50031 insertion site. Lines which did not show amplification in one or both reactions were chosen for further analysis. Figure 6, panels A and B, show selected results from this initial scan. Shown here are six reactions that were carried out with each primer set including, a positive control (OR), four test lines (EY*4, GE89, GE77 and GE*69), and a negative control (no DNA).

PCR of the wild type strain (OR) shows amplification of bands of the expected size in both cases. Imprecise excision was indicated in the case of EY*4, GE89 and GE77. This was determined by the absence of amplification with the downstream set of primers (panel B) in the case of EY*4, GE89 and GE77, as well as, no amplification of GE77 with the upstream set of primers (panel A). The EY*4 line was obtained from a parallel excision experiment conducted with the EY2625 P-element insertion line by our collaborators in France (Maryvonne Mével-Ninio, personal communication). GE77 and GE89 were isolated from the GE50031 P-element excision scheme carried out by me.

To determine the exact deletion breakpoints of these putative deletions additional sets of primers were employed. The results of these experiments are shown in Figure 6 C. The sequences obtained from sequencing analysis of each line are included in the appendix.

*The EY*4 deletion spans 1269bp and deletes the first predicted ATG of the DIP1 gene.*

The breakpoints of the EY*4 deletion were determined by amplification with primers ML1751 and AB28564. In the wild type (OR) this primer set spans a 2Kb region (Figure 6C lane 1). However, in EY*4 these primers amplified a band of only 650bp (Figure 6C lane 2) indicating a deletion of approximately 1Kb. Sequencing of the PCR fragment confirmed the presence of a 1269bp deletion with breakpoints at the point of the EY2625 P-element insertion (+23) and at the proximal end of the second exon (+1293) (Figure 4B).

The GE89 deletion spans 2Kb and deletes both putative ATG sites and the proximal end of the bipartite NLS.

Another primer set, ML9006 and ML11487, was used to amplify the breakpoints of the GE89 excision Amplification of the GE89 strain with these primers resulted in a 1.5Kb band (Figure 6C, lane 3). The expected size of the region spanned by these two primers is 3.45Kb. Thus, it appeared that a deletion of approximately 2Kb had occurred. Sequencing of the 1.5Kb band confirmed a deletion of 2Kb with breakpoints at the point of the GE50031 P-element insertion (+23) and at the proximal end of the second intron (+1918) (Figure 4B). This deletion removes several important motifs that have been predicted to be part of the *DIP1* gene including, both predicted translation start sites (+122 and +1615) and the 5' end of the predicted NLS (+1764 - +1797).

The GE77 deletion spans 2.8Kb of the 5' regulatory region of the DIP1 gene.

Finally, the breakpoints of the GE77 deletion were also determined. In this case primers ML13631 and ML13632 were used to amplify an approximately 650bp band from the GE77 line (Figure 6C, lane 4). In the wild type genome these two primers span a region of 3 812bp. A deletion of 3Kb was confirmed by sequencing with breakpoints in intron 1 (+709) and 2450bp upstream of the 5' end of *DIP1* (Figure 4B). This deletion

removes the entire first exon including the first putative ATG as well as more than 2Kb of the upstream regulatory region.

P-element excision GE8 was identified as a precise excision of the GE50031 element.

As a control for phenotype analysis excision GE8 was identified as a precise excision of the GE50031 element. PCR of this line with primers ML1751 and AB28564 amplified the expected size band of 2Kb. Subsequent sequencing of the PCR product determined that the DNA sequence in this line had indeed been returned to its original form. This was confirmed by clustalw alignment of the obtained sequence with the sequence published by NCBI (AE003122.5)

*Further PCR analysis of EY*4, GE89 and GE77 identified disruptions of several putative motifs of the DIP1 gene: However, in all strains the dsRBDs remain intact.*

Previous analysis of the *DIP1* gene found it to contain two putative translation start sites as well as, two dsRBDs (Pelka, Masters Thesis, 2000, De Sousa *et al.,* 2003). Also, an *in vitro* assay was done to confirm that DIP1 does indeed act like a dsRNA-binding protein (Pelka, Masters Thesis, 2000, De Sousa *et al.,* 2003). Overall, the presence of these motifs in the *DIP1* transcript may be considered very important for the proper functioning of the *DIP1* gene. Thus, to identify if any of these sites were disrupted by the above described deletion strains further PCR analysis was undertaken. Firstly, primers AB28564 and AB28563 were paired together to amplify a 500bp region of the *DIP1* gene that encodes the second predicted translation start site (ATG_2). Figure 6D shows the results of this experiment. Strain GE89 was shown to be missing ATG_2 due to a lack of amplification with this pair of primers (Figure 6D, lane 3). However, this domain remains in tact in all other strains that were examined (Figure 6D, lanes 2, 4 & 5). As well, a pair of primers was designed to amplify a 1Kb region spanning both dsRBDs (ML9004, ML9005). This pair of primers amplified the expected size band (1Kb) in all cases (Figure 6E).

Overall, three deletions of the *DIP1* gene were molecularly characterized (Figure 4B). The first of these deletions, EY*4, deletes the first predicted translation start site while leaving the second one in tact. This may indicate that this allele affects some *DIP1*

isoforms but not others. The GE89 deletion is a more extensive deletion and may have a more severe impact on *DIP1* gene expression. Finally, GE77 is different from the other deletions in that it removes the regulatory region of the *DIP1* gene. In order to investigate the impact of each of these deletions on *DIP1* gene expression I characterized the pattern of DIP1 protein expression by immunohistochemistry.

Immunohistochemistry of ovaries from *DIP1* deletion strains reveals patterns of staining that differ from the wild type.

Immunohistochemistry of ovaries using an anti-DIP1 antibody was used to determine if the three newly derived *DIP1* deletion strains have altered DIP1 protein staining. Previous characterization of DIP1, by Dorothy De Sousa, has established a consistent wild type protein expression pattern (De Sousa *et al.*, 2003). This standard was used for comparison to results outlined in this section.

*Anti-DIP1 antibody staining of EY*4 ovaries did not differ from wild type.*

Firstly, the DIP1 staining pattern in ovaries from the EY*4 strain were looked at. Figure 7 shows the results of this experiment. Panels A and C show the wild type (OR) while EY*4 is shown in panels B and D. The left column of Figure 7 (panels A & C) represents a medial plane of focus while the right column is a more proximal focal plane. The wild type is characterized by punctate staining in the nuclei of both the nurse cells and the follicle cells. Nurse cells are shown here located in the bottom right quadrant of all panels. Distinct punctate staining of the large nuclei of these cells is clearly visible in the wild type (panels A & B). When the nurse cells were examined at a higher magnification (lower left inset panel B) spots of staining along the edges of the cells representing ring canals also became apparent. The upper right inset in panel B shows a higher magnification view of the follicle cells. These are somatic cells which cover the area of the ovariole where the developing oocyte is located. Punctate staining was clearly visible in these cells. Careful examination of the EY*4 staining pattern did not show any apparent deviation from the wild type pattern. Punctate staining of the nuclei in both the nurse cells and the follicle cells was apparent (panels C & D). Higher magnification

examination of both the nurse cells and follicle cells also revealed a staining pattern indistinguishable from that of the wild type (insets panel D).

Immunohistochemistry of GE89 ovaries presents inconclusive results.

The DIP1 staining pattern of the GE89 *DIP1* deletion strain was also investigated. The results from this experiment were inconclusive. Two rounds of staining were conducted with differing results in each case. Ovaries from the first round of staining were found to have very little staining suggesting DIP1 protein expression had been ablated in the GE89 strain. Some staining found in the ring canals was also noted. A second round of anti-DIP1 antibody staining produced a very different result. A significant amount of staining was observed in the nuclei of both the nurse cells and follicle cells. It was interesting to note that a few egg chambers appeared to have irregularly shaped nurse cells. However, in some late stage egg chambers the morphology and staining pattern was indistinguishable from the wild type. Blind comparison of GE89 and wild type ovaries stained with anti-DIP1 antibody from each of these two batches was undertaken. In this experiment four slides of each strain were observed. All of the GE89 slides were identified as differing from wild type, while one of the wild type slides was misidentified. Given the discrepancy in staining results between the two immunohistochemistry experiments described here, it is impossible to determine the exact nature of the DIP1 expression pattern in GE89 ovaries. Ultimately, another round of immunohistochemistry is required before any conclusions can be made.

Staining of controls for the GE89 and GE77 deletions revealed reduced follicle cell staining in the original GE50031 P-element insertion line.

For comparison purposes ovaries were dissected and stained from several control strains including: wild type, the original GE50031 P-element insertion (GE) and a precise excision (GE8). Also, as a negative control, wild type ovaries were dissected and stained with secondary antibody only. The results of these experiments are shown in Figure 8 (OR panels A & B, GE panels C & D, secondary only panels E & F, GE8 panels G & H). The upper row shows a superficial focal plane while the bottom row shows a deeper focal plane.

Firstly, anti-DIP1 antibody staining of OR ovaries recapitulated the wild type DIP1 expression pattern. Also, the pattern of staining observed in the precise excision (panels G & H) closely resembles that of the wild type. Distinct nuclear staining in both the follicle cells and nurse cells was visible. As well, strong staining of the ring canals was observed (lower left inset panel G). As a negative control, staining with the secondary antibody only was also done. Any staining visible in this case was limited to a faint ubiquitous outlining of the cells (Figure 8, panels E & F). No specific nuclear staining was detected. In addition, higher magnification examination of these samples did not reveal any further staining (insets panels E & F).

Interestingly, anti-DIP1 antibody staining of ovaries from the original GE50031 (GE) P-element insertion revealed a staining pattern that differed from that of the wild type (Figure 8, panels C & D). Staining of the nurse cells appeared to follow the wild type pattern of punctate nuclear staining (panel D & inset panel D). However, the follicle cells appeared to be lacking specific DIP1 staining (panel C & inset panel C). This inconsistency between the wild type staining pattern and that of the GE50031 P-element insertion strain may warrant further investigation in the future.

In general, a wild type pattern of DIP1 staining was established for the GE50031 precise excision strain (GE8). As well, an intriguing lack of staining in the follicle cells of ovaries from the GE50031 P-element insertion strain was observed. It will be interesting to further investigate this apparent tissue specific lack of staining.

GE77 ovary morphology differed from wild type and is reminiscent of the morphology of the BG2658 insertion.

Finally, the DIP1 staining pattern of ovaries from the GE77 *DIP1* deletion strain was investigated. The results of this experiment are shown in Figure 9. In comparison to the wild type (panels A & B) GE77 (panels C &D) was found to have a very similar staining pattern including punctate nuclear staining of the nurse cells (panel C, deeper focal plane) and follicle cells (panel D, superficial focal plane) as well as specific staining of the ring canals (inset panel C). It was also interesting to note that the overall morphology of the GE77 ovaries was somewhat disrupted. The ovaries dissected from

this strain were generally smaller, more rounded and more delicate than those from wild type strains. This aberrant morphology is similar to that observed previously in the BG2658 P-element insertion strain (Jen Kinder undergraduate thesis, 2003). Immunohistochemistry of ovaries from the BG2658 strain are shown in Figure 9 panels E & F as an example. Panel E shows a medial focal plane in which specific staining of the nurse cell nuclei was observed. Also, a superficial focal plane of the same ovariole is shown in panel F. Distinct nuclear staining of the follicle cells was observed at this level of focus. However, unlike the wild type this ovariole is rounded and the nurse cells did not appear to be characteristically arranged. The relationship between the GE77 *DIP1* deletion strain and the BG2658 P-element insertion line will be discussed further below.

Overall, the results of this set of experiments looking at the anti-DIP1 staining pattern in the ovary suggest some differences in the expression of DIP1 in the GE50031 P-element insertion strain and the GE77 deletion strain.

Is *DIP1* required for female fertility?

Previously, the BG2658 P-element line inserted 1.6Kb upstream of the 5' end of *DIP1* was found to be homozygous female sterile (Jen Kinder, Undergraduate Thesis, 2003, Table 3). To date it has not been confirmed if this sterility phenotype maps to the *DIP1* gene. However, it should be noted that there are no other predicted open reading frames within at least 150 000bp 5' of *DIP1* (Figure 4A). This supports the hypothesis that the sterility phenotype is associated with disrupted *DIP1* gene function.

Recently, one of the deletions obtained from the GE50031 P-element mutation scheme, GE77, was also found to be homozygous female sterile (Table 3). Analysis of the breakpoints of the GE77 excision indicated that the region of the genome where the BG2658 insertion was located had been removed (Figure 4B). Complementation crosses between these two lines showed that heterozygotes were viable (Table 3). The sterility of the GE77/BG2658 heterozygotes was tested by crossing twenty individual females to FM7j/Dp(1;Y) males and incubating them at 25°C. After 20 days six of these females were found to have reproduced. In each of these cases no more than 10 adult flies were collected. As well, no apparent phenotypes were observed in those flies that did eclose.

Although specific analysis was not conducted, neither the GE89 deletion nor the GE50031 P-element insertion lines showed a sterility phenotype. An investigation of viability of the GE77, GE89 and GE50031 lines with a deficiency line shown to uncover *DIP1* (Df(1)LB6) did not indicate even a low level of lethality (Table 3). In all cases, the affected chromosome over Df(1)LB6 occurred with a similar frequency to a balancer control. Only one line, PE16, which is lethal both homozygous and over Df(1)LB6 has been isolated to date. PE16 is a P-element insertion line positioned 5' of the BG2658 insertion in the 5' regulatory region of *DIP1* isolated in a previous P-element mobilization scheme (Jen Kinder, Undergraduate Thesis, 2003)

In summary, it appears that the BG2658 female sterile P-element insertion line and the GE77 female sterile *DIP1* deletion line do not completely complement each other. This result suggests that the sterility in both cases may be occurring due to a disruption of the same element. Overall, it appears that there may be a role for the *DIP1* gene in female ovary development and/or fertility.

Is *DIP1* required for proper appendage development?

Upon beginning to work with the GE50031 P-element insertion line some interesting phenotypes were observed. As GE50031 is inserted in the 5' end of the *DIP1* gene it was considered possible that these phenotypes were occurring due to a disruption or alteration of DIP1 expression. Thus, characterization of these phenotypes, including establishing the frequency of occurrence and recording images of the altered structures, was undertaken.

The most commonly observed phenotypes were leg duplications and disruptions of leg structures. Examples of these phenotypes are recorded in Figure 10. The images in the left column were taken at 10x magnification while the images in the right column were taken at a higher magnification (20x). A wild type leg is included for comparison (panels C & D). Panels A & B show a small duplication of the tarsi. Duplication of a few or all of the tarsi, similar to that shown here, was the most frequently observed phenotype. Less frequently larger duplications, loss of appendages and severely altered leg morphology were also observed. Panels E and F show a severely altered leg. In this

case the leg was thickened and shortened with what appears to be an additional claw and possibly other duplicated structures. In general, leg phenotypes were observed in some but not all legs of the affected flies. However, the phenotypes did not seem to occur more frequently in any particular appendage.

Overall, leg duplications and disruptions of leg morphology were observed in 3% of hemizygous males (Table 2). When the GE50031 P-element insertion line was looked at in females over a deficiency known to delete *DIP1* the frequency of these phenotypes increased to 15% (Table 2). A Y-chromosome carrying a duplication of a region of the X-chromosome was added to the background the observed phenotype frequency was reduced to 1.5% (Table 2). As a control, a precise excision line derived from GE50031 was also checked for the presence of leg phenotypes. <1% of these flies were observed to have severe leg phenotypes (Table 2). Also, addition of a duplication that carries the *DIP1* gene to the precise excision did not alter the observed phenotype notably. However, when the precise excision was examined with a deficiency known to delete *DIP1* in the background the frequency of the phenotypes increased slightly to 4% (Table 2). Chi Squared analysis of the frequency data indicated a large variation from expected values only in the case of GE50031/Df(1)LB6 (χ^2 107.436).

The GE50031 P-element line was obtained from a Korean database of P-element insertions (GenExel, http://genexel.com/eng/htm/genisys.htm). Their annotation of the GE50031 element indicates that it is an EP element oriented such that the UAS promoter, in the presence of GAL4, would drive expression in the direction opposite to the direction of *DIP1* transcription. Thus, it was suspected that the observed leg phenotypes may have arisen from leaky expression at the UAS promoter. To further investigate this hypothesis, the GE50031 P-element insertion line was combined with several GAL4 lines at 29°C. However, none of the GAL4 elements investigated further altered the viability or phenotype of the GE50031 line (data presented in the appendix).

Leg duplications and severe disruptions of leg morphology appear to occur significantly more frequently in the GE50031 insertion strain than would be expected. It is also interesting to note, that similar appendage phenotypes have been observed in the

GE89 and GE77 *DIP1* (Jen Kinder & Jessica Jackson) deletion lines although the frequency of these occurrences has not been documented. The frequency of these occurrences also seems to be reduced by precise excision of the P-element. However, further data including observations of wild type flies is required to determine if DIP1 is required for proper appendage development.

Repeat induced mini-white gene silencing is altered by disruptions of *DIP1* gene expression.

Previous research characterizing the *DIP1* gene has pointed towards a role for DIP1 in epigenetic mechanisms of gene regulation. In order to begin testing this hypothesis, the effects of several *DIP1* deletions on gene silencing were investigated. Firstly, a repeat induced mini-white gene silencing paradigm was used. In this assay, fly strains carrying repeats of a P{lacW} transposon which exhibits a variegated eye pigment expression pattern were used. Previously, additions of mutations of genes from the RNAi pathway, as well as genes known to play a role in chromatin remodeling or structure formation have been shown to alter the pigment variegation of these strains (Dorer and Henikoff, 1994). We were interested in determining if similar results would be found with deletions of the *DIP1* gene. The results reported in this section were collected for the most part by Jessica Jackson as part of her fourth year thesis project and a summer research project. My role in this experiment was to help set up the protocol, act as an advisor to Jessica and work in co-operation with Jessica to help collect some of the data.

The effect of the EY*4 DIP1 deletion and the GE50031 P-element insertion on repeat induced silencing was investigated. For this investigation strains of flies carrying tandem and inverted repeats of the mini-white gene were obtained. Two of these strains, BX1 and DX1, were looked at in combination with both the EY*4 deletion and the GE50031 insertion. Spectrophotometer absorbance measurements were taken of both the control and the test strains at a wavelength of 480nm. Preparations for quantitative measurements were made by emulsion of 15 fly heads (aged three days post eclosion) in an acidified solution of methanol. The results of these measurements are reported in graphical form (Figure 11). Little to no pigment was measured in the wild type, EY*4, or

GE insertion strains not carrying any copies of the mini-white gene arrays. As well, very little pigment was quantified in the BX1 and DX1 mini-white array lines with w^{1118} backgrounds as mini-white gene expression in these lines is silenced. However, when both the BX1 and the DX1 array lines were combined with the EY*4 deletion eye pigment expression significantly increased (Figure 11). ANOVA statistical analysis followed by Tukey's pairwise comparisons found EY*4; BX1 and EY*4;DX1 to be significantly different from BX1 and DX1 respectively. By contrast, no significant differences between GE;BX1 or GE;DX1 and the original strains were found.

Qualitative comparisons of eye pigment in the EY*4;BX1 and EY*4;DX1 lines to the original strains also followed the same trend. Figure 12 shows images of the eyes of representative examples from the BX1 and EY*4;BX1 lines. Panels A and B show mini-white gene expression in a wild type background. Whereas, panels C and D show mini-white gene expression when the EY*4 *DIP1* deletion is in the background. The images in the top row were taken at a lower magnification. In these panels it is interesting to note the variability of mini-white gene expression among flies of the same genotype. Comparison of the higher magnification images of BX1 to EY*4/BX1 indicated a dramatic increase in pigment in the case of the EY*4 background.

Heterochromatic white gene silencing is altered by disruptions of DIP1 gene expression.

The X-inversion paradigm was also used to look further at the effects of the EY*4 and GE89 deletions of the *DIP1* gene on gene silencing. A precise excision of the GE50031 P-element (GE8) was also included as a control. In this paradigm, expression of the white gene follows a variegating pattern due to an inversion of the X-chromosome that juxtaposed the white gene to a region of constitutive heterochromatin (Schotta et al., 2003). Mutant alleles of genes involved in formation and maintenance of heterochromatin have been shown to alter the variegating pattern of white gene expression. Previously, two alleles of the PEV gene Su(var)3-9 have been shown to reduce heterochromatic gene silencing in this paradigm (Tschiersch *et al*, 1995). As an interaction between DIP1 and Su(var)3-9 has been suggested by a yeast-two hybrid

screen (Krauss *et al.*, 2000), it was of interest to see if the deletions of the *DIP1* gene also reduced heterochromatic gene silencing. Also, a possible interaction between Su(var)3-9 and the DIP1 alleles with regards to heterochromatic gene silencing was investigated by combining both elements together with the In(1)w[m4] chromosome.

*No interaction was found between Su(var)3-9 and the EY*4 and GE89 DIP1 alleles in the X-chromosome inversion paradigm.*

Figure 13 shows the amount of eye pigment production in yw/In(1)w^{m4} increased significantly with both Su(var)3-9^1 and Su(var)3-9^2 in the background in comparison to a balancer control. Measurements were also made for EY*4/In(1)w^{m4}, GE89/In(1)w^{m4} and GE8/In(1)w^{m4} in combination with both Su(var)3-9 alleles (Figure 13). For each strain a minimum of two quantitative measurements were taken (15 flies each) from which, the mean value and standard error of the mean were calculated. The mean values are plotted in Figure 13. A one-way ANOVA followed by Tukey's pairwise comparisons was carried out in order to compare the different groups. Results from this analysis indicated that, EY*4/In(1)w^{m4};Su(var)3-9^1 had significantly higher pigment than the yw control. However, this result was not repeated with the second Su(var)3-9 allele. Instead, the GE89 *DIP1* deletion with Su(var)3-9^2 showed significantly increased pigment from the yw/In(1)w^{m4};Su(var)3-9^2 control. It should also be noted that the pigment expression of the precise excision control (GE8) was not significantly different from yw in the case of either Su(var)3-9^1 or Su(var)3-9^2. Despite the measurement of statistically different quantities of eye pigment in several cases, the trend portrayed by graphing these results shows a clustering of values for Su(var)3-9 alone and in combination with EY*4, GE89 and GE8. Thus, it is unlikely that there is any functional interaction between the alleles of DIP1 tested here and Su(var)3-9.

The GE89 deletion of the DIP1 gene significantly increases eye pigment expression in the X-chromosome inversion paradigm.

Although no interaction between Su(var)3-9 and DIP1 was found with regards to decreasing silencing of the In(1)w^{m4} element, it was of most interest to analyze the effect of each *DIP1* gene deletion on In(1)w^{m4} alone. The results of this experiment are

presented in Figure 14. To start with, very little pigment was detected in the wild type control (yw/In(1)w^{m4} Figure 14). As well, analysis of EY*4/In(1)w^{m4} did not show a significant increase in pigment expression. By contrast, the eye pigment quantification of GE89/In(1)w^{m4} showed a significant increase in pigment expression. Measurement of the GE8/In(1)w^{m4} control was also significantly greater than the wild type background. However, the amount of pigment quantified in this case was still significantly less than in the case of GE89. Measurements for this experiment were made in a manner similar to that described for the Su(var)3-9 interaction experiment described above. Also, a one-way ANOVA followed by Tukey's pairwise comparisons was carried out in order to compare the different groups. This analysis confirmed that both GE89/In(1)w[m4];TM3,Sb,Hu flies and GE8/In(1)w[m4];TM3,Sb,Hu flies expressed significantly more eye pigment protein than the yw control. It should also be noted, that the quantity of pigment measured in the case of the precise excision GE8/In(1)w[m4] was significantly less than that quantified for the *DIP1* deletion allele GE89/In(1)w[m4].

Overall, it appears that the different *DIP1* deletion strains have an affect on both repeat induced silencing and position effect variegation. However, this effect is not straight forward and further investigation is required to look more closely at a possible function for DIP1 in the silencing pathway.

Figure 2: Induction of recombinant DIP1 protein and purification by Ni-NTA His-tag affinity column.

Panel A: Coomassie stained SDS-PAGE gel of DIP1a pET29b+ BL21(DE3) protein induction from time 0 to 5 hours. A distinct band of DIP1a protein becomes visible at 3 hours. Peak expression of DIP1 is seen at 4.5 hours. Arrow indicates DIP1a protein.

Panel B: Coomassie stained SDS-PAGE gel of the washing steps from Ni-NTA affinity purification of His-tagged DIP1a protein. Arrow indicates level at which DIP1a protein is observed. DIP1a protein is observed in the induced control. As well, DIP1 protein is observed in the flow through (FT) and washes at pH6.5 and pH6.2.

Panel C: Coomassie stained SDS-PAGE gel of the elution steps from Ni-NTA affinity purification of His-tagged DIP1a protein. DIP1a protein is detected in the induced control (I ctrl) and flow through (FT) lanes. As well, a small amount of purified DIP1a protein was eluted at pH4.0

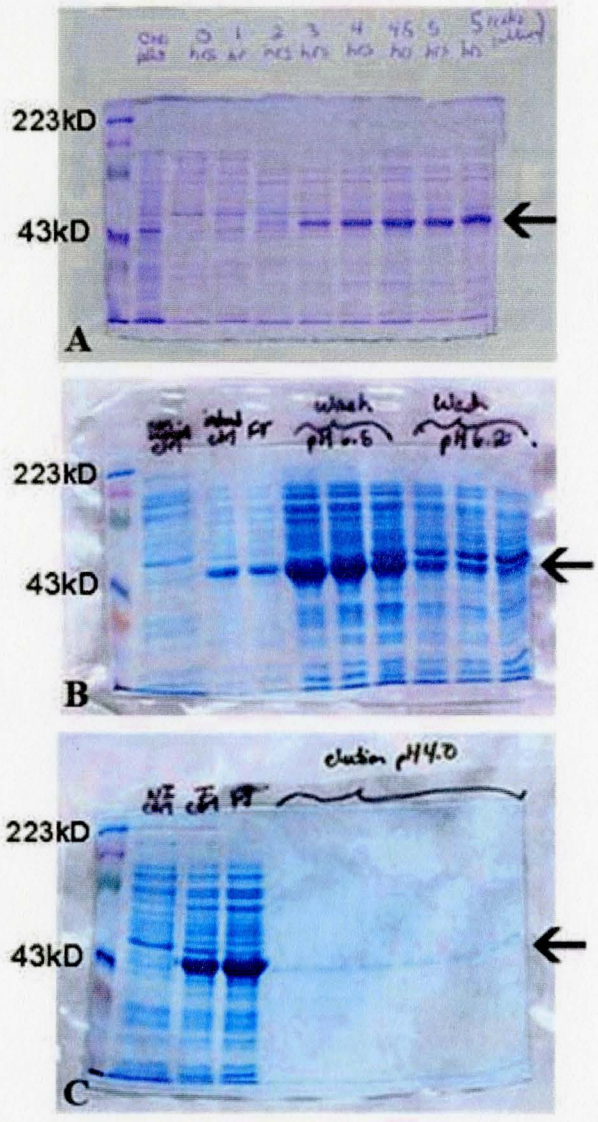
223kD
43kD
A
223kD
43kD
B
223kD
43kD
C

Figure 3: DIP1a protein purified by gel electro-elution and confirmed as His-tagged DIP1 by Western blot.

Panel A: Coomassie stained SDS-PAGE gel of DIP1a protein purified by gel electro-elution. DIP1a protein, as well as many other bacterial proteins, is seen in the cleared lysate (CL). Lane E is the eluate. Following the gel electro-elution procedure purified DIP1a protein was eluted from the other proteins.

Panel B: Western blots detected with anti-DIP1 polyclonal antibody and anti-His antibody respectively. DIP1 protein was detected by anti-DIP1 antibody in both cleared lysate (CL) and eluate (E). Anti-His antibody also recognized a protein at the expected size of DIP1 in the eluate. This indicates that the His-tag on the DIP1a protein is in tact.

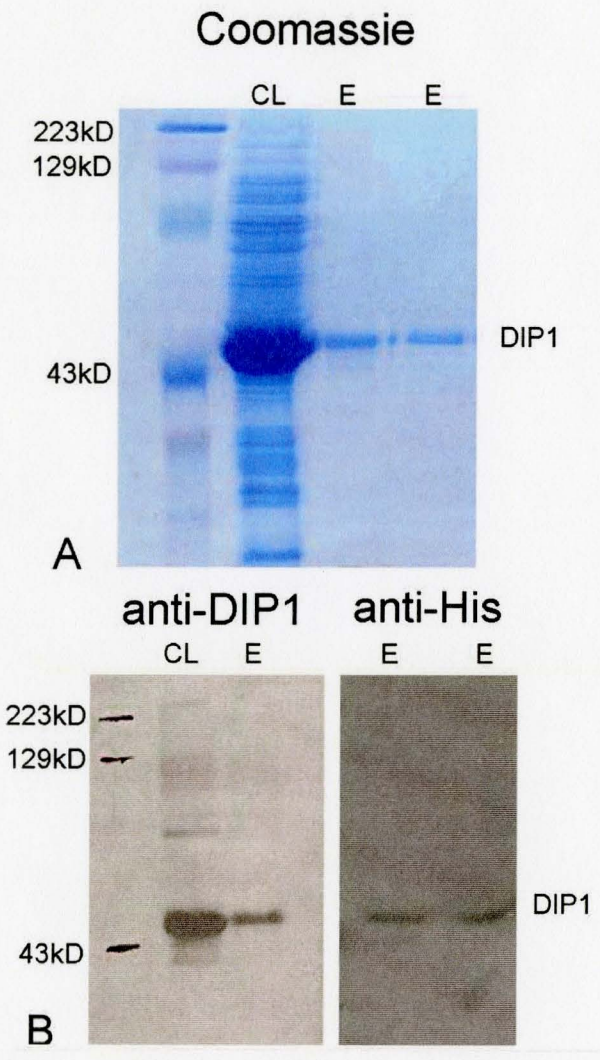
Coomassie
CL
E
E
223kD
129kD
43kD
DIP1
A
anti-DIP1
anti-His
CL
E
E
E
223kD
129kD
43kD
DIP1
B

Figure 4: Genomic organization and annotation of the *DIP1* gene and surrounding genome.

Panel A: Representation of the 20A-20B region of the *Drosophila melanogaster* X-chromosome as depicted on the FlyBase Genome Browser available at: http://flybase.bio.indiana.edu/cgi-bin/gbrowse_fb/dmel. Predicted genes are depicted as light blue arrows with their mRNA isoforms shown in darker blue. In this representation, the *DIP1* gene can be found in the centre with its 5' end to the right and 3' end to the left. Each tick mark on the base ruler demarks 10Kb. Note that in the region directly 5' of *DIP1* there are no predicted genes within approximately 200Kb.

Panel B: Higher magnification representation of the *DIP1* gene. Specific features of the *DIP1* gene as well as primer locations and P-element insertion points are depicted here. Primers are shown as arrows indicating their direction and approximate location. Further details with regards to exact location and sequence are provided in the appendix. The locations of all features are denoted by base pair relative to the 5' end of *DIP1* (0) as determined from the genome sequence available from NCBI (AE003122.5). The general structure of *DIP1* is made up of 4 exons. Three different isoforms identified previously in the Campos lab are generated from differential splicing of the first intron. Another significant isoform was identified that lacks the NLS (Bondos et al., 2004) but is not shown here. Two putative translation start sites were predicted (ATG_1: +122 & ATG_2: +1615). As well, the *DIP1* gene encodes a bi-partite NLS (+1764 - +3285) as well as two dsRBDs (dsRBD1: +3321 - +3521 & dsRBD2: +3813 - +4079). Also shown here is a representation of the breakpoints of three lines which delete portions of the *DIP1* gene. EY*4 deletes a region 1269bp long with breakpoints +23 and +1293. The GE89 line has breakpoints +23 and +1918 which represent a deletion of 2Kb. Finally, GE77 is a 3Kb deletion with breakpoints -2450 and +709. Sequences of each breakpoint analysis are included in the appendix.

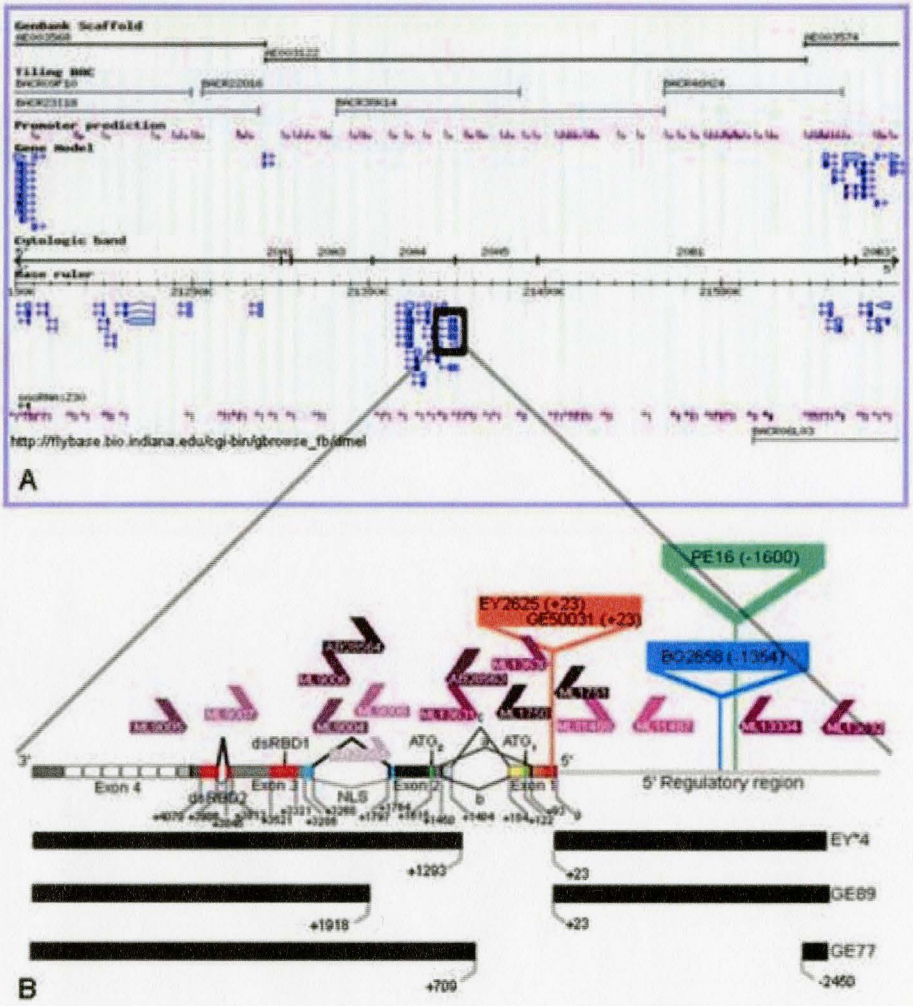
GenBank Scaffold
Tiling BAC
Promoter prediction
Gene Model
Cytologic band
Base ruler
http://flybase.bio.indiana.edu/cgi-bin/gbrowse_fb/dmel
A
PE16 (-1600)
EY2625 (+23)
GE50031 (+23)
EO2658 (-1354)
dsRBD1
dsRBD2
NLS
Exon 4
Exon 3
Exon 2
Exon 1
5' Regulatory region
EY*4
GE89
GE77
+1293
+1918
+709
+23
+23
-2460
B

Figure 5: General crossing scheme for P-element mediated mutation of *DIP1*.

Initially, a transposase source was crossed to females carrying a P-element insertion in proximity to *DIP1* (see Figure 4). The combination of these two elements enables excision and re-insertion of the P-element. In the F1 an X-chromosome balancer was crossed in to stabilize potential mutations and prevent crossing over from occurring. Single female progeny from the F1 cross were selected based on eye colour (white eyes indicated removal of the P-element which carries a mini-white marker). To establish broods of unique excision events, single females were crossed to males with a duplication of part of the X chromosome onto the Y chromosome balanced with FM7. Thus, hemizygous/homozygous lethal excisions were not lost. Molecular analysis of each brood was conducted using an established set of PCR primers (see Figure 4) and DNA sequencing.

P1: Transposase source *(w/Y;+/+;ry506, Sb, P{Δ2-3,ry}99B/TM6B,Tb,Hu)*♂

× P-element strain virgin females♀

F1: P-element + transposase*

× X-chromosome balancer *(FM7)* homozygous virgin females♀

**Excision events occur in the germline of these males*

Select single white eyed virgin females*♀

× *duplication of X on the Y (Dp(1:Y)) over an X-chromosome balancer (FM7)*♂

**Create broods of unique excision events*

Analyze the breakpoints of each unique excision event by PCR & Sequencing

Figure 6: PCR analysis of potential DIP1 excision characterized three deletions of the *DIP1* gene.

Panel A: Primers ML11486 and ML11487 were designed to amplify a 500 bp region of the genome 5' of the GE50031/EY2625 P-element insertion site. A 500bp band was amplified from the wild type (OR), GE89 and GE*69. Lack of amplification of a specific band from GE77 indicates a deletion of the region of the genome 5' of *DIP1*.

Panel B: Primers AB28564 and ML1750 were used to amplify a 1.8Kb region 3' of the EY2625/GE50031 P-element insertion site. Lack of amplification from the EY*4, GE89 and GE77 strains indicates deletions of the 5' end of the *DIP1* gene.

Panel C: For each deletion strain specific primer pairs were used to amplify across the deletion breakpoints. Primers ML1751 and AB28564 amplify a 2Kb region of the wild type genome (OR). The same primers amplify only 650bp from the EY*4 strain. Primers ML9006 and ML11487 amplified a 1.5Kb band from GE89 compared to the 3.45Kb span of the wild type genome. A 650bp band was amplified from the GE77 strain with primers ML13631 and ML13632 designed to span 3 812bp of the wild type genome.

Panel D: Primers AB28564 and AB28563 were used to amplify the region of the *DIP1* gene that encodes the second predicted ATG. The expected band of 500bp was amplified from all strains except GE89.

Panel E: A set of primers, ML9004 and ML9005, which span both dsRBDs of the *DIP1* gene amplified the expected 1Kb band in all cases.

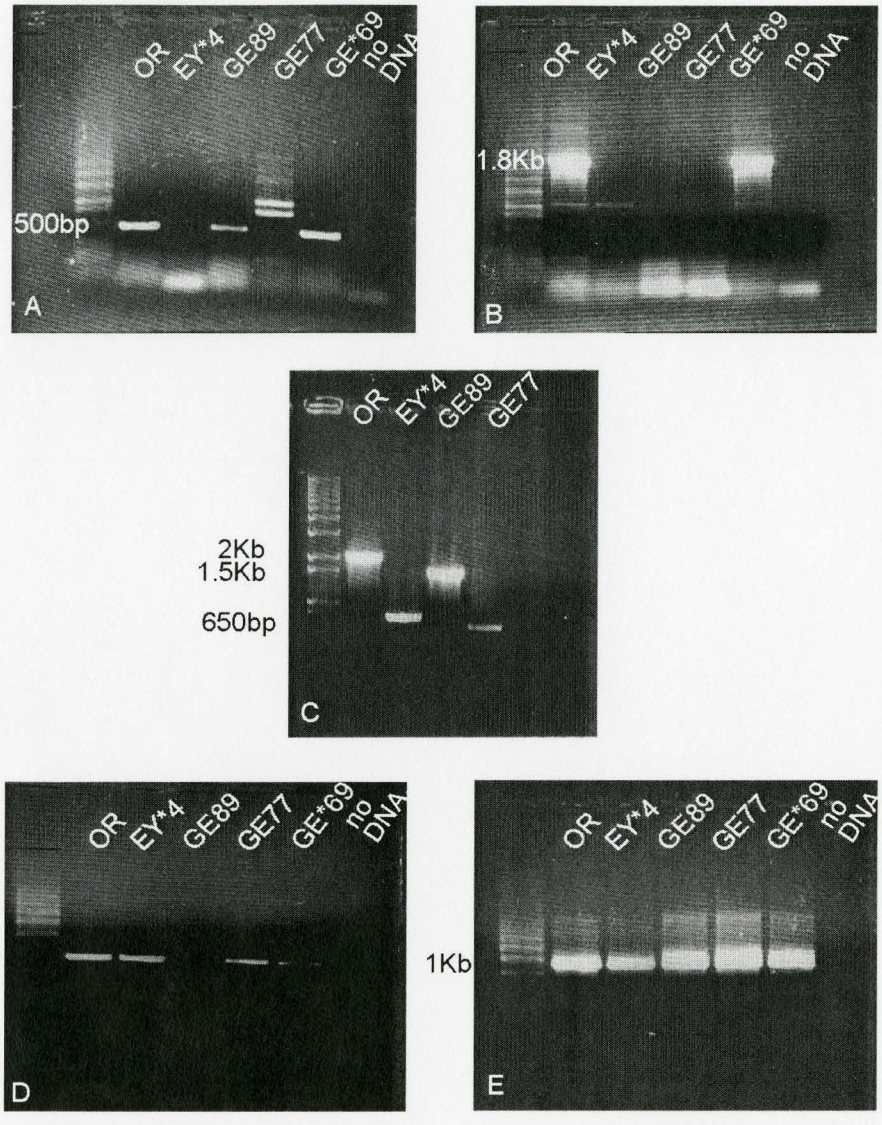
OR
EY*4
GE89
GE77
GE*69
no DNA
500bp
A
1.8Kb
B
2Kb
1.5Kb
650bp
C
500bp
D
1Kb
E

Figure 7: Immunohistochemistry of ovaries from the EY*4 strain shows no difference from wild type.

The ovaries from wild type (OR) and EY*4 were stained with anti-DIP1 polyclonal antibody and visualized by confocal microscopy (20X magnification). Panels A and B show labeling of OR ovaries at a medial (A) and more superficial (B) plane of focus. Punctate nuclear staining is seen in both the nurse cells and the follicle cells. Distinct points of staining are also seen along the membrane of the nurse cells in structures known as ring canals. The lower let inset in panel B shows a 40x magnification of the nurse cells and gives a clearer view of ring canal staining. A higher magnification view (40x) of the follicle cells show more clearly that DIP1 staining is not ubiquitous in the nucleus but instead is localized to distinct subdomains. Similarly, panels C and D show labeling of EY*4 ovaries at a medial (C) and more superficial (D) focal plane. Nurse cell and follicle cell nuclei are stained in a pattern indistinguishable from wild type. A higher magnification (40X) view of the follicle cells (inset in panel D) shows the wild type pattern of localization to subdomains. Distinct ring canal staining is also seen (40X inset panel D)

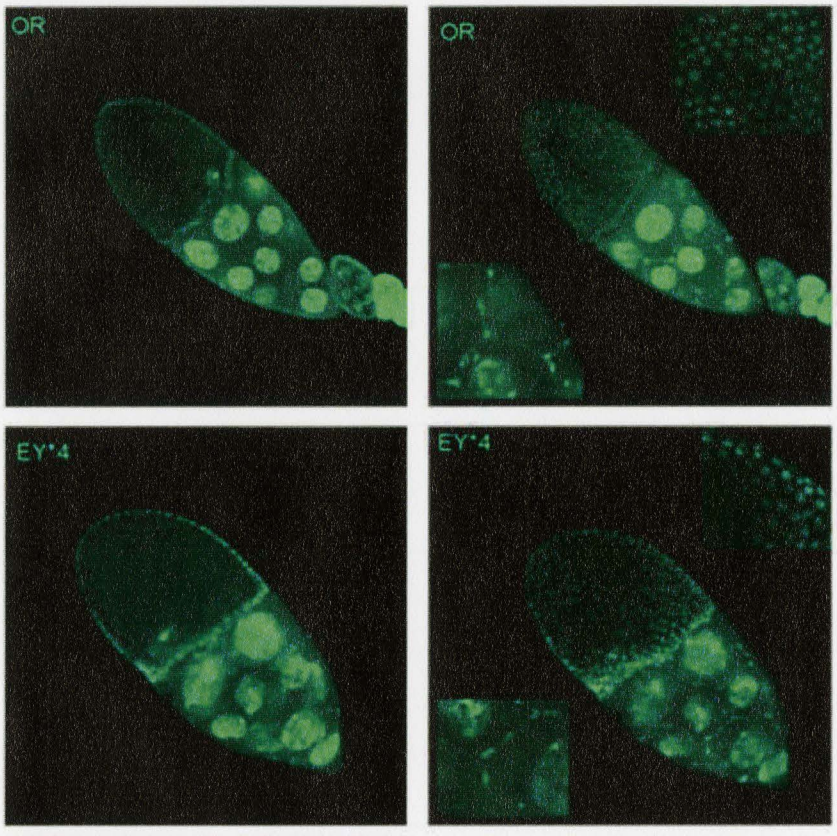
OR
OR
EY'4
EY'4

Figure 8: The DIP1 staining pattern of the GE89 *DIP1* deletion ovaries differs from that of the wild type.

Confocal images of late stage egg chambers stained with anti-DIP1 polyclonal antibody. All images were taken at 20X magnification with insets at 40X magnification. Panels A, C, E, G and I are of a superficial focal plane, while panels B, D, E, H and J are of a more medial plane of focus.

Panels A & B: labeling of wild type (OR) ovaries. A more complete description of the wild type staining pattern can be found in Figure 7.

Panels C & D: labeling of ovaries from the GE50031 P-element insertion line. Staining in the nurse cells of these egg chambers resembles wild type (panel D and panel D inset). Visualization of the follicle cells shows a lack of staining (panel C and panel C inset).

Panels E & F: labeling of wild type ovaries with secondary antibody only as a negative control. No specific staining is seen in this case.

Panels G & H: labeling of ovaries from GE8 a precise excision strain included as a positive control. A wild type pattern of DIP1 expression is observed with distinct nuclear staining seen in both nurse cells and follicle cells. Higher magnification views (insets panel I) also show a wild type staining pattern with localization of DIP1 staining to subdomains in follicle cells as well as distinct staining of the ring canals.

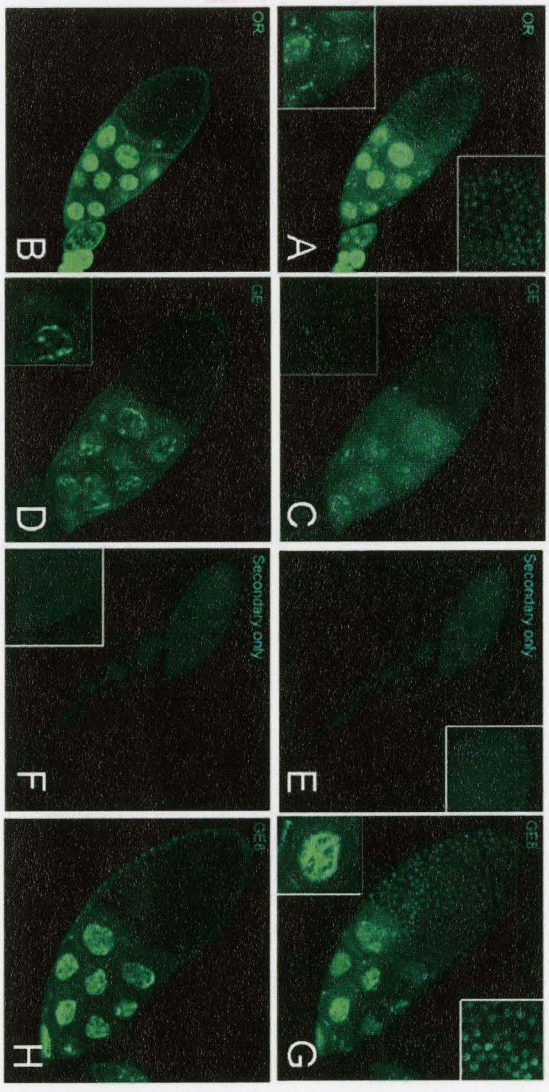
A
OR
B
OR
C
CE
D
CE
E
Secondary only
F
Secondary only
G
CE
H
CE

Figure 9: Ovaries dissected from the *DIP1* deletion strain GE77 have a pattern of DIP1 staining similar to wild type and also exhibit aberrant morphology.

Confocal images of OR and GE77 late stage egg chambers were visualized with anti-DIP1 polyclonal antibody staining at a medial (A & C) and more superficial (B & D) focal plane. A more complete description of the wild type staining pattern can be found in Figure 7. Anti-DIP1 staining of GE77 ovaries shows distinct nuclear staining of the nurse cells (C) and follicle cells (D). Higher magnification views (40X) of the nurse cell region show specific staining of the ring canals (inset C). A 40X magnification look at the follicle cells (inset D) also shows wild type like punctuate staining localized to subdomains.

Panels E & F: epi-fluorescence images of ovaries from the BG2658 P-element insertion strain. A view of the medial focal plane (E) shows nuclear staining of nurse cells while a more superficial view (F) shows punctuate follicle cell staining. Staining of these egg chambers appears to follow a wild type pattern although the morphology of these egg chambers differs. Images of BG2658 ovaries are included for comparison purposes in describing the altered morphology of ovaries from the GE77 strain.

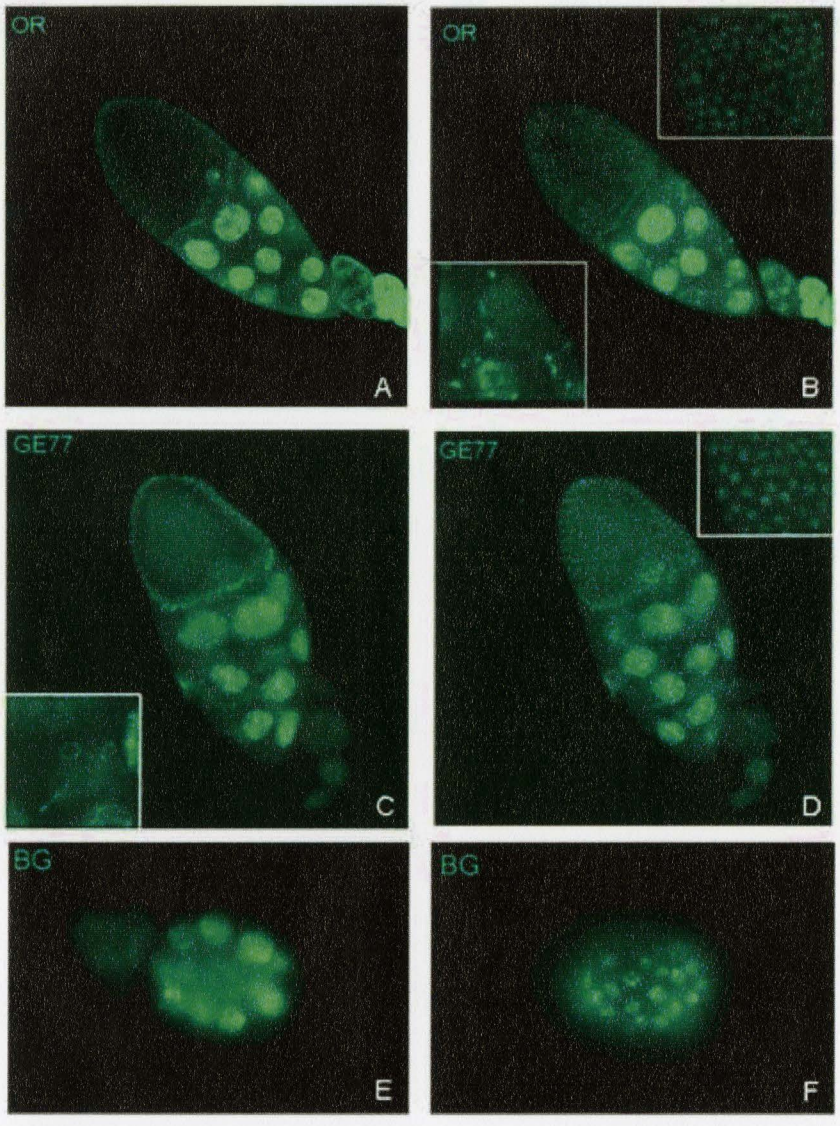
OR
A
OR
B
GE77
C
GE77
D
BG
E
BG
F

Figure 10: Leg duplications and disrupted leg morphology observed in GE50031 P-element insertion line.

Panels A-F show legs dissected from GE50031 flies and visualized by light microscopy at a magnification of 10X (A, C, E) or 20X (B, D, F).

Panels A & B: leg duplication of the three most distal tarsi.

Panels C & D: normal leg development

Panels E & F: disrupted leg morphology. A duplicated claw is visible (arrow) as well as the overall appearance of the leg is thickened.

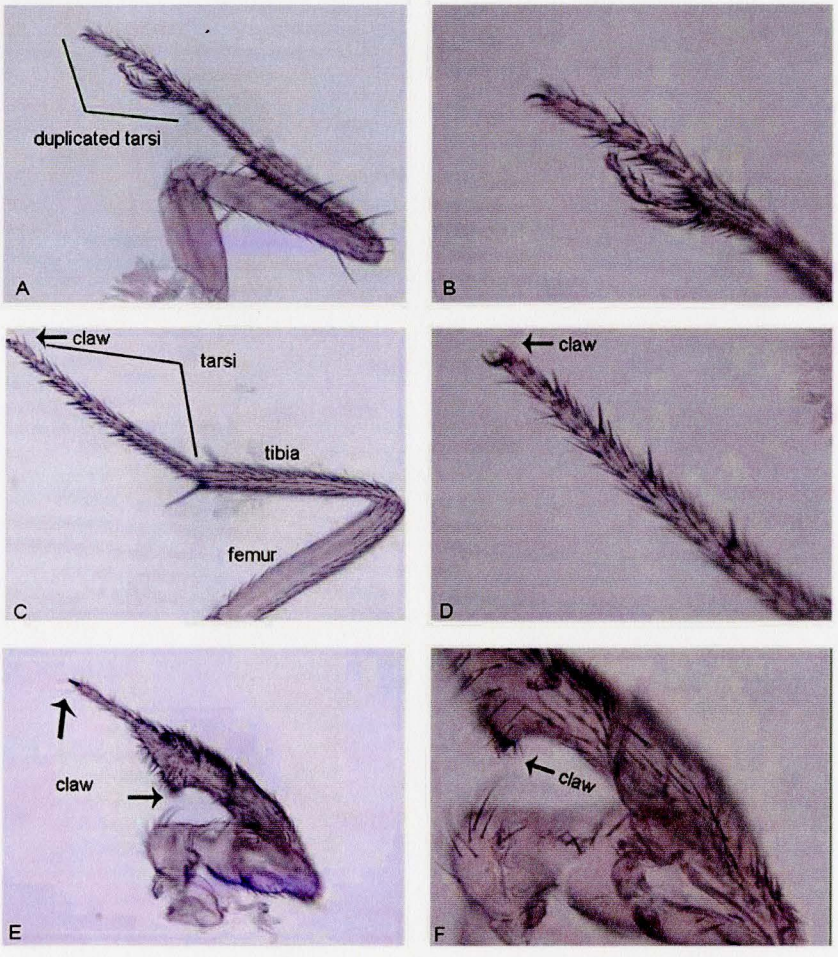
duplicated tarsi
A
B
claw
tarsi
tibia
femur
C
claw
D
claw
E
claw
F

The results presented in Figures 11, 12 and 14 were collected by Jessica Jackson. The heads of 15 flies, aged three days post eclosion, were emulsified in acidified methanol. A spectrophotometer was used to measure the absorbance of the solution at a wavelength of 480nm. Three separate measurements were taken for each genotype and the mean absorbance value was plotted graphically. Error bars represent the standard error of the mean. One-way ANOVA analysis followed by Tukey's pairwise comparisons was done to identify significant interactions.

Figure 11: Eye pigment quantification in Repeat Induced Silencing Paradigm

Comparison of the EY*4/Y;BX1/BX1 measurement of eye pigment to that of the BX1 array in a wild type background shows a significant difference (ANOVA $p<0.001$). Similarly, EY*4/Y;DX1/DX1 has a significantly higher eye pigment concentration than the DX1 array alone (ANOVA $p<0.001$). Measurements for both EY*4/Y and GE50031/Y were taken as controls. A small amount of eye pigment was quantified in the GE50031 strain due to mini-white gene expression from the P-element insertion. A significant change in eye pigment expression was not detected for GE50031/Y;BX1/BX1 or for GE50031/Y;DX1/DX1.

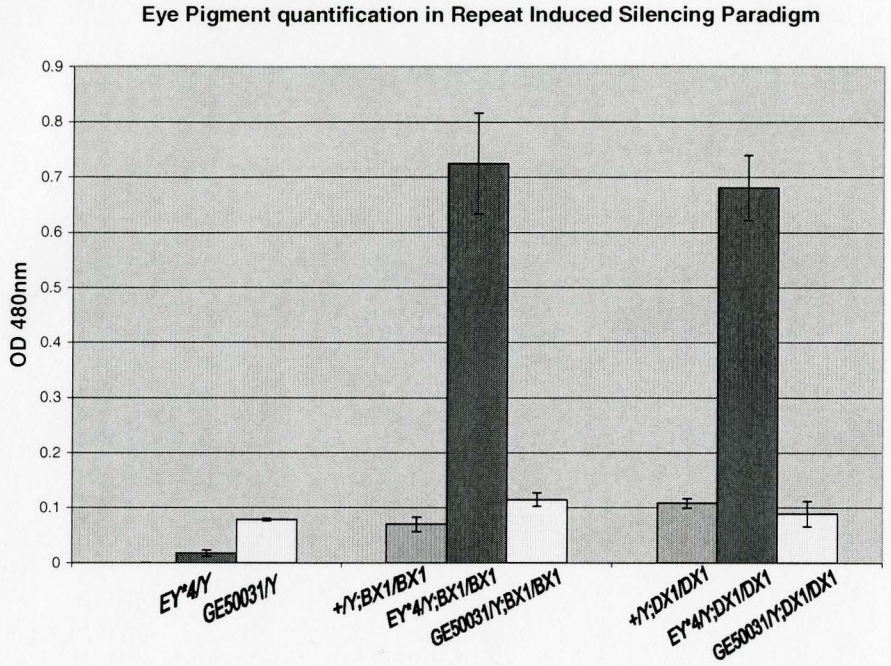
Eye Pigment quantification in Repeat Induced Silencing Paradigm
OD 480nm
0.9
0.8
0.7
0.6
0.5
0.4
0.3
0.2
0.1
0
EY*4/Y
GE50031/Y
+/Y;BX1/BX1
EY*4/Y;BX1/BX1
GE50031/Y;BX1/BX1
+/Y;DX1/DX1
EY*4/Y;DX1/DX1
GE50031/Y;DX1/DX1

Figure 12: Qualitative examination of eye colour shows an increase in eye pigment expression in the EY*4/Y;BX1/BX1 line compared to BX1 alone.

Brightfield microscopy images of whole fly heads from the mini-white array line BX1 compared to EY*4/Y;BX1/BX1.

Panels A & B: yw/Y;BX1/BX1 eyes have variegated patches of eye pigmentation. Panel A shows two fly head at a low magnification demonstrating the variability in eye pigment expression observed in this fly strain. Panel B is a higher magnification view. Particular pigmented and non-pigmented spots can be seen.

Panels C & D: EY*4/Y;BX1/BX1 eyes have much larger and more prominent patches of red pigmentation. Panel A comparison of two flies with the same genotype demonstrates that some variability in eye pigment expression was observed. Panel B is a higher magnification view enabling visualization of the apparently darker eye pigmentation and larger patches of white gene expression.

Crosses by: Jessica Jackson
Images by: Jennifer Kinder

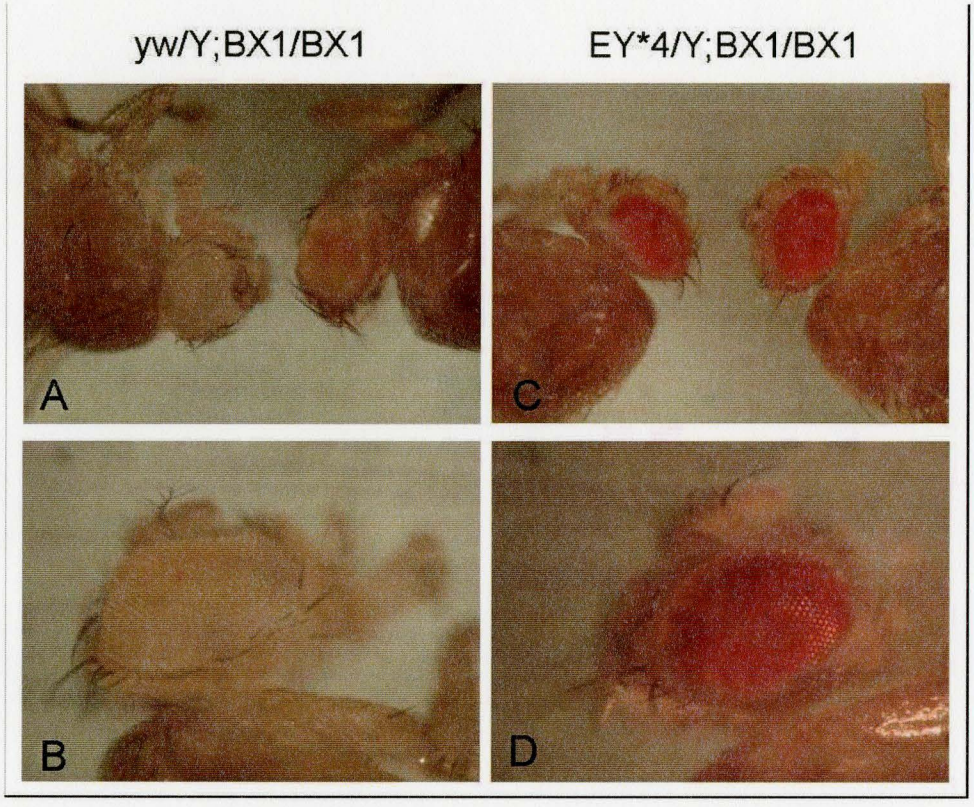
yw/Y;BX1/BX1
EY*4/Y;BX1/BX1
A
C
B
D

Figure 13: Eye pigment quantification of X-chromosome inversion interaction with Su(var)3-9.

A much higher quantity of eye pigment was measured for yw/In(1)w^{m4};Su(var)3-9^1 and yw/In(1)w^{m4};Su(var)3-9^2 flies in comparison to a balancer control yw/In(1)w^{m4};TM3,Sb,Hu (ANOVA, $p<0.001$). Measurements for each allele of Su(var)3-9 in combination with EY*4, GE89 and GE8 strains cluster around the same value.

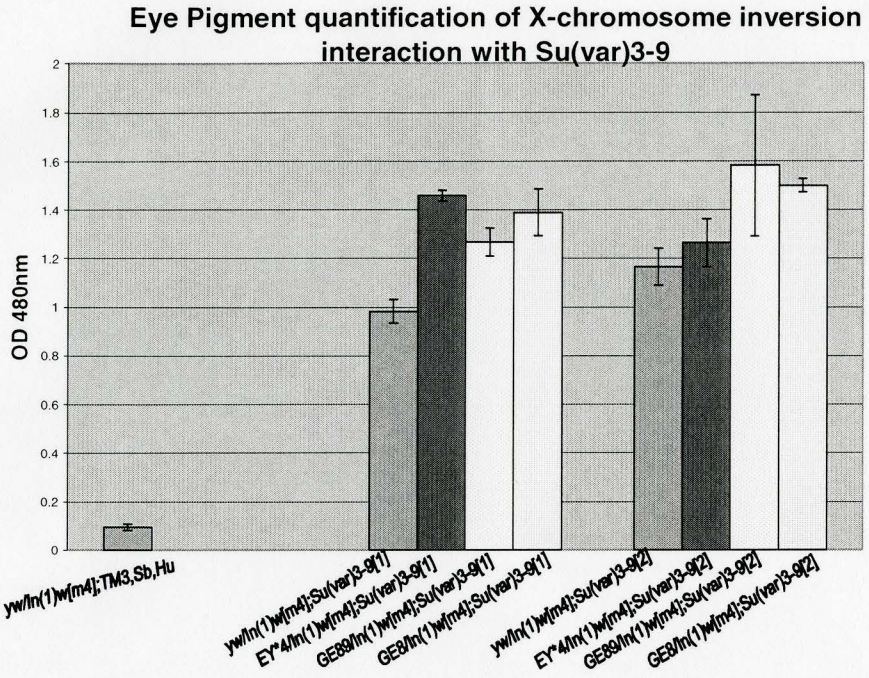
Eye Pigment quantification of X-chromosome inversion interaction with Su(var)3-9
OD 480nm
2
1.8
1.6
1.4
1.2
1
0.8
0.6
0.4
0.2
0
yw/In(1)w[m4];TM3,Sb,Hu
yw/In(1)w[m4];Su(var)3-9[1]
EY*4/In(1)w[m4];Su(var)3-9[1]
GE89/In(1)w[m4];Su(var)3-9[1]
GE8/In(1)w[m4];Su(var)3-9[1]
yw/In(1)w[m4];Su(var)3-9[2]
EY*4/In(1)w[m4];Su(var)3-9[2]
GE89/In(1)w[m4];Su(var)3-9[2]
GE8/In(1)w[m4];Su(var)3-9[2]

Figure 14: Eye pigment quantification of X-chromosome inversion interaction with DIP1 alleles.

A small quantity of eye pigment expression was measured in control, yw/In(1)w^{m4};TM3,Sb,Hu, flies. EY*4/In(1)w^{m4};TM3,Sb,Hu flies did not show a significant increase in pigment compared to the control strain. A significant increase in eye pigment expression was measured for the GE89/In(1)w^{m4};TM3,Sb,Hu strain compared to control flies (ANOVA, $p<0.001$). A significant increase in eye pigment expression was also measured for the GE8/In(1)w^{m4};TM3,Sb,Hu precise excision strain compared to the control strain and to GE89/In(1)w^{m4};TM3,Sb,Hu.

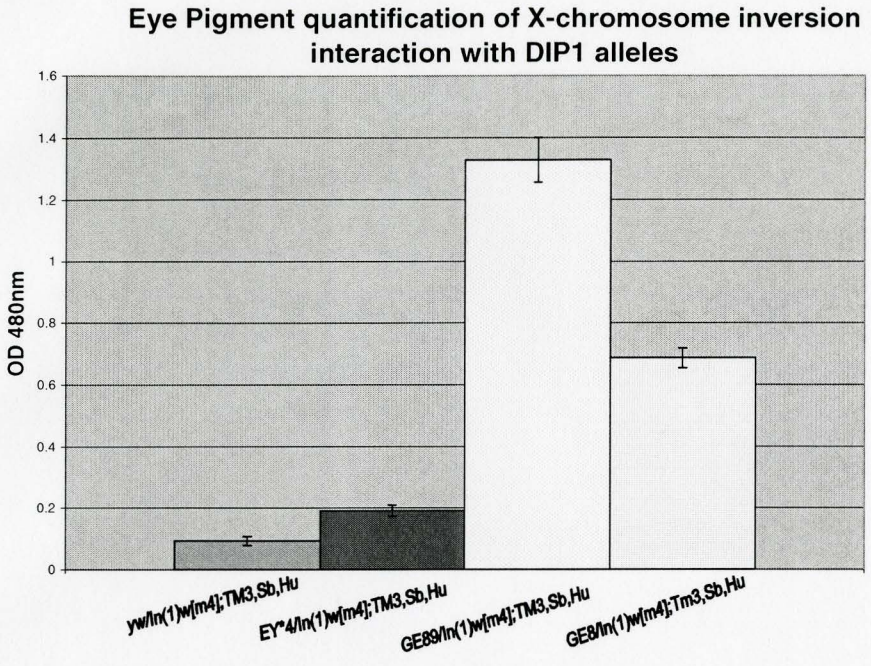
Eye Pigment quantification of X-chromosome inversion interaction with DIP1 alleles
OD 480nm
1.6
1.4
1.2
1
0.8
0.6
0.4
0.2
0
yw/In(1)w[m4];TM3,Sb,Hu
EY*4/In(1)w[m4];TM3,Sb,Hu
GE89/In(1)w[m4];TM3,Sb,Hu
GE8/In(1)w[m4];Tm3,Sb,Hu

	BG2658 Mobilization¶	EY2625 Excision	GE50031 Excision
# possible excisions/ mobilizations screened	1374	857	Data not collected
# potential excisions/ mobilizations identified & investigated	24	24	100
# imprecise excisions established	NA	0	2
Rate of excision	2%	3%	NA

Table 1: Counts showing frequency of excision
¶Results previously presented (Kinder, Undergraduate Thesis, 2003)

A low rate of P-element excision (2%-3%) was observed for several P-elements inserted into the genome near the 5' end of the *DIP1* gene. Observation of such a low rate of excision from the first two rounds of mutagenesis indicated a much larger scale screen was necessary to increase the likelihood of identifying a *DIP1* deletion. 148 lines that appeared to be potential P-element excisions or mobilizations affecting the *DIP1* gene were isolated. Of these, two lines have been characterized as deletions of the 5' end of the *DIP1* gene.

Genotype	% Occurrence of aberrant appendages
GE50031/Df(1)LB6	15% (43/280)
GE50031/Y	3% (84/2602)
GE50031/Dp(1:Y)	1.5% (3/207)
GE50031 Precise Excision (GE8)	<1% (.72%) (2/276)
GE50031 Precise Excision/Dp(1:Y)	1% (.97%) (3/310)
GE50031 Precise Excision/ Df(1)LB6	4% (3.85%) (11/286)

Table 2: Observed Frequency of leg phenotypes

Genotype	Lethal	Sterile
BG2658/BG2658¶	No BG/Y (808):FM7/Y (499)	Yes (of 20 females none produced progeny)
GE77/BG2658	No GE77/BG(73):BG/FM7(59)	Yes (of 20 females 6 produced < 10 progeny)
GE77/GE77	No	Yes (of 20 females none produced progeny)
GE77/Df(1)LB6	No GE77/Df(22):GE77/FM6(21)	ND
GE89/Df(1)LB6	No GE/DF(79):GE/FM6(93)	ND
GE50031/Df(1)LB6	No GE/Df(79):GE/FM6(93)	ND
PE16/PE16¶	Yes	-
PE16/Df(1)LB6¶	Yes	-
PE16/BG2658¶	No	Yes (low level of fertility observed)
EY*4/Df(1)LB6	No EY*4/Df(250):EY*4/Dp(221)	ND
EY2625	No EY/EY(336):EY/Dp(328)	ND

Table 3: Complementation tests of viability and sterility phenotypes

¶ Data in these rows was presented previously
(Jen Kinder, Undergraduate Thesis, 2003)

ND – Not Determined

Chapter IV
Discussion

Mutagenesis of the *DIP1* gene: Resistance to mutation.

Limitations of P-element mediated mutagenesis and possible alternative methods for DIP1 specific mutation.

P-element transposition is an extremely useful technique which has been harnessed to place a large number of genes in the *Drosophila* genome under experimental control (Bellen et al., 2004). As of March 2004, the BDGP gene disruption project had associated specific P-element insertions with approximately 40% of all predicted genes in *Drosophila melanogaster* (Bellen et al., 2004). This is a significant increase from the 25% reported in 1999 (Spradling et al., 1999). For the most part, this increase can be attributed to the completion of the *Drosophila* genome sequencing project. The availability of the annotated *Drosophila* genome has enabled determination of each P-element insertion site by sequence analysis; eliminating the need for time consuming polytene chromosome *in situ* hybridization and complementation analysis (Bellen et al., 2004). A search of the BDGP gene disruption database identified two P-element insertion lines associated with the *DIP1* gene.

P-element transposition has targeted a wide region of the genome for insertional mutagenesis. However, P-element insertion is a non-random event with preference for insertion into the 5' end, or promoter regions, of genes (Tower et al., 1993). As well, certain genes seem to be elusive targets for P-element insertions. There is evidence to suggest that P-elements may recognize specific DNA structures rather than DNA sequences as preferred insertion sites (Liao et al., 2000). The two elements currently identified in the BDGP database as associated with the *DIP1* gene are both located in the 5' end (BG2658 1Kb upstream, EY2625 in 5'UTR) (http://flystocks.bio.indiana.edu/). Although there may be a disruption of *DIP1* gene expression by these elements, it would also be useful to have an element inserted in the *DIP1* open reading frame (orf). Considering our current understanding of P-element transposition and experience with the *DIP1* region of the *Drosophila* genome, it appears unlikely that a P-element will insert directly into the *DIP1* open reading frame.

Another transposable element, the *piggyBac* element, has recently been under investigation as an alternative to the P-element (Bonin and Mann, 2004,Hacker et al., 2003). Inactivation of individual genes and subsequent functional analysis is the focus of many *Drosophila* geneticists; including our investigation of the *DIP1* gene. The *piggyBac* element has been proposed to facilitate such investigations. This element, unlike the P-element, appears to be less susceptible to inserting into hot spots. Excision of this element, also unlike the P-element, looks to occur most frequently without altering the original point of insertion (Hacker et al., 2003). It has also been shown that *piggyBac* elements insert preferentially into introns and generally show insertion site preferences that differ from those of P-elements (Hacker et al., 2003).

One group of researchers (Bonin and Mann, 2004) has developed a *piggyBac* element intended to exploit the frequent insertion of these elements into introns. In this case, a *piggyBac* element was fused with an EGFP reporter and a transcriptional termination sequence. Flies heterozygous for insertion of this element into an intron will express EGFP in an insertion site specific manner, while flies homozygous for this element will eliminate gene expression via termination of transcription. Another group of researchers (Hacker et al., 2003) have also established that transposition of *piggyBac* elements does not alter the integrity of stably integrated P-elements. Thus, the two transposition mechanisms can be used in a complementary manner and together will facilitate more complete functional analysis of the *Drosophila* genome by inactivation of specific genes. Further, establishment of a *piggyBac* database similar to the BDGP P-element gene disruption database will certainly aid functional analysis of the *Drosophila* genome.

With regards to analysis of the *DIP1* gene, it will be advantageous should a *piggyBac* element insertion associated with the *DIP1* gene become available. However, a level of success of disrupting *DIP1* expression has been attained with P-element mediated mutagenesis. Thus, in the short term, it is likely to be more profitable to continue to focus on P-element mediated disruption of the *DIP1* gene.

Low rate of P-element excision at DIP1 locus is a consequence of its location in the genome and mechanisms of P-element induced DSB repair.

The observed rate of excision for P-elements associated with the *DIP1* gene was approximately 2%-3%. This rate is relatively low compared to the rate of excision reported for similar elements located elsewhere in the genome (personal communication, Niko Pretorious). It is most likely that the low rate of excision around the *DIP1* gene is due to its proximity to a region of heterochromatin. It has been shown that restriction enzyme digestion of P-element constructs inserted into areas of heterochromatin is impaired (Wallrath and Elgin, 1995). By extension, it is likely that transposase enzyme activity would also be reduced in areas of heterochromatin.

A low rate of deletions associated with P-element excisions was also observed. This is likely similar to the rate of imprecise excisions relative to general excisions in other areas of the genome and is a consequence of Double Strand Break (DSB) repair mechanisms. P-element mediated DSB repair has been shown to occur by homologous recombination (Engels et al., 1990, Reviewed in McVey et al., 2004). The Synthesis-Dependent Strand Annealing (SDSA) model suggests a mechanism for this process (Nassif et al., 1994). This model can explain many of the outcomes of P-element excision including: P-element duplication, incorporation of sequence from a sister strand (Nassif et al., 1994), internal P-element deletion (Kurkulos et al., 1994) and deletions of adjacent DNA (Ma et al., 2003). In general, immediately following P-element excision the remaining DNA site is characterized by a double stranded DNA break. Repair of this DSB is required to maintain the integrity of the genome. The first step of repair following a DSB involves digestion by a 5'-3' exonuclease (Reviewed in Ma et al., 2003). The single stranded 3' ends then seek out and invade homologous sites (Nassif et al., 1994). DNA is synthesized from the 3' end using the homologous site as a template. Ultimately, pairing occurs between regions of homology between the newly synthesized single stranded DNA. Completion of this process using a sister strand as a template can result in restoration of the DNA to exactly the same state as prior to excision and the DSB (Nassif et al., 1994). Alternatively, the single stranded 3' end may immediately recognize

a homologous site on the opposite 3' free end. Subsequent annealing of these regions and gap filling may result in a deletion any where from a few base pairs to more than several hundred base pairs (Ma et al., 2003).

Several adjustments to our genetic scheme for generating P-element mediated mutations of the *DIP1* gene were made to maximize the probability of imprecise excision. Firstly, the scheme was set up such that transposition took place in the germline of male flies. In this case there is no homologous chromosome that can be used as a template for DSB repair. Also, transposition was suggested to occur more frequently at a lower temperature (personal communication, Marc Therrien). Thus, developing embryos in which transposition may occur were kept at 19°C. Recently, several genes involved in the integrity of DSB repair have been identified (McVey et al., 2004). It may be useful to consider conducting P-element mutagenesis with mutations of these genes in the background as a way to increase the rate of the desired outcome from P-element excision.

Three novel deletions of the *DIP1* gene have three unique impacts on *DIP1* gene expression.

Considerable insight into the function of a gene can be gained from observation of its mutant phenotype. Thus, a null mutation of the *DIP1* gene would greatly facilitate the investigation of the function of this gene. P-element mutagenesis of the *DIP1* gene yielded several interesting deletion alleles (EY*4 generated by Maryvonne Mével-Ninio, GE89 and GE77 generated by me). While none of these deletions eliminated the *DIP1* coding region completely, they were nevertheless useful to initiate a dissection of the *DIP1* gene function.

*The EY*4 deletion is an isoform specific deletion of DIP1-b and -c.*

Firstly, the EY*4 deletion removes the first exon. A portion of this exon is translated into *DIP1* isoforms DIP1b and DIP1c (Pelka, 2000). However, the entire coding region for the DIP1a isoform remains intact. This suggests that the EY*4 deletion is an isoform specific deletion which may retain wild type like function of the DIP1a isoform. Results from immunohistochemistry experiments support the suggestion that some DIP1 protein expression remains (Figure 7). Anti-DIP1 polyclonal antibody

staining of ovaries from the EY*4 strain revealed a wild type pattern of DIP1 expression. If it does in fact hold true that EY*4 is an isoform specific mutation it may be worth staining other tissues at different developmental stages to look for a possible isoform specific pattern of expression.

The GE89 deletion appears to disrupt the 5' portion of each of the identified isoforms of DIP1.

Another deletion, GE89, deletes a larger portion of the 5' end of the *DIP1* gene. In this case, the coding regions for the N-terminus of each of the known isoforms of the *DIP1* gene, DIP1-a, -b and -c (Pelka, 2000) as well as DIP1-d (Bondos et al., 2004), were deleted. Based on this evidence, it was predicted that there would be no DIP1 protein expressed in this strain. Testing of this hypothesis by immunohistochemistry experiments was inconclusive. Staining of GE89 ovaries with anti-DIP1 antibody resulted in a range of results from very little staining to staining that more closely resembles the wild type pattern. Although no specific conclusions can be drawn from these data it seems that at least some specific anti-DIP1 staining can be seen in GE89 ovaries. This observation appears to refute the hypothesis that DIP1 protein expression is abolished in the GE89 deletion strain. Alternatively, as a portion of the coding region of the *DIP1* gene remains intact, it is also possible that the GE89 strain may produce some truncated protein.

Translation start sites are identified *in vivo* by the small (40S) ribosomal subunit which scans the mRNA from the 5' end and comes to rest at the first appropriate ATG site (Kozak, 1996). Thus, deletion of the upstream sequence may reveal a previously undetected ATG site such that a truncated protein may be formed. The initiator codon for protein translation must be an ATG or closely related codon such that it is recognizable by the Met-tRNA as this is the only tRNA able to initiate protein synthesis (Reviewed in Kozak, 1996). As well, a consensus motif for the context of a strong translation initiation site has been established (GCCACCatgG Reviewed in Kozak, 1996). Recently, ATGpr, was identified as the most reliable web tool available to identify ATG translation start sites (Nadershahi et al., 2004). Analysis of the remaining genomic sequence in the GE89 deletion with this tool may prove useful towards characterizing this allele.

In addition, the GE89 deletion affects one half of the bipartite NLS. Nuclear localization signals are recognized by carriers in the cytoplasm and subsequently transported through the nuclear pore complex into the nucleus (Reviewed in Nigg, 1997). An alteration of the integrity of the NLS may compromise nuclear import of any DIP1 protein that may be formed. Therefore, it may be reasonable to expect at least a reduction of nuclear DIP1 expression in tissues from the GE89 strain. However, monopartite NLSs have also been identified (Reviewed in Nigg, 1997). Consequently, the collection of basic residues at the 5' end of exon 3 may be sufficient to signal nuclear import of a truncated protein synthesized from a GE89 transcript.

Taken together the evidence discussed above supports the hypothesis that, while the 5' ends of each of the known DIP1 protein products have been affected by the GE89 deletion there may not be a visible change to anti-DIP1 antibody labelling. A Northern blot or RT-PCR assay would be useful to determine whether a truncated mRNA transcript of DIP1 is being formed in the GE89 strain. Similarly, Western analysis of protein extracts from the GE89 strain would identify if any truncated DIP1 protein has been produced. As a final note, it is important to recall that detection of a truncated protein produced in the GE89 deletion strain does not provide any information about the functionality of this protein.

*The GE77 deletion is similar to the EY*4 allele with an additional deletion of the 5' regulatory region.*

GE77, similar to the EY*4 deletion, deletes the first exon while the second ATG remains in tact. In addition, approximately 2Kb of the upstream regulatory region was also deleted in this strain. Immunohistochemistry of ovaries from the GE77 deletion strain revealed a wild type pattern of DIP1 protein expression (Figure 9). This result is consistent with the findings for EY*4. However, it should be noted that the morphology of the ovaries dissected from the GE77 deletion strain was abnormal.

In conclusion, three novel alleles of the *DIP1* gene have been characterized. Each of these alleles is a deletion, to varying degrees, of the 5' end of the *DIP1* transcript. The availability of these alleles has greatly improved our ability to address questions

regarding the function of the *DIP1* gene. However, the generation of a completely molecular and genetic null of the *DIP1* gene is still required.

Disruption of the regulatory region directly 5' of the *DIP1* gene results in female sterility and altered ovary morphology.

The 5' region disrupted by both the BG2658 P-element strain and the GE77 DIP1 deletion strain likely represents a germ cell or ovary specific regulatory region.

Two of the lines described in this report, GE77 and BG2658, displayed a female sterile phenotype (Table 3). The effects of these mutations appear to be limited to germ cell formation and/or development as the overall morphology of the adult fly seems otherwise unaffected. Molecular characterization of these two lines demonstrated a common area of disruption in the 5' regulatory region of *DIP1* in both these strains. As described above and shown in Figure 4, BG2658 is a P-element insertion strain with an insertion site approximately 1Kb upstream of the *DIP1* transcription start site. GE77 is a deletion strain that eliminates the first exon of the *DIP1* gene as well as approximately 2Kb of the 5' regulatory region including the BG2658 insertion site. Complementation analysis of these two strains demonstrated that they do not fully complement (Table 3). Therefore, we concluded that sterility in both lines arises from disruption of the same element. Perhaps sterility in both cases can be attributed to disruption of a tissue or cell specific enhancer resulting in down regulation of *DIP1* expression in the female ovary.

Currently, our ability to define and recognize a cis-regulatory element by genome inspection is limited (Istrail and Davidson, 2005). However, these regions are extremely important for producing specific patterns of gene expression regulated in space and time. Action at specific regulatory regions as well as combinatorial effects between actions at multiple regulatory regions can lead to tightly controlled temporal and/or spatial gene expression (Levine and Davidson, 2005). Tissue and cell-specific regulatory sequences have been identified in many genes. For example, the β2 tubulin gene in *Drosophila* has been shown to have a 14bp promoter element that controls its male germ cell-specific expression (Michiels et al., 1989). In order to identify this promoter element, deletion constructs of the 5' regulatory region of the β2 tubulin gene were fused to a *lacZ* reporter

and transformed into flies. As well, long range promoter elements, required in cis, have also been identified. In mice, an interesting example of Sonic hedge hog regulation was identified in which limb specific regulation was controlled by a regulatory element located 1Mb away from the Shh coding sequence in the intron of another gene (Sagai et al., 2005).

It is clear that developing an understanding of the regulatory sequences of a particular gene and their specific roles is a complex process. These elements can lie at a significant distance from the transcriptional unit which they control and do not have distinct and identifiable genomic characteristics. In the case of DIP1 it appears that both GE77 and BG2658 disrupt an ovary or germ cell specific regulatory element. This is supported by the fact that these are two independently isolated mutations in the region of the *DIP1* gene which display a similar tissue specific phenotype. However, further investigation is required to define the regulatory region of the *DIP1* gene.

Establishment of a specific role for the miRNA pathway in germ cell development may also suggest a role for DIP1.

Development of the *Drosophila* ovary follows a distinct set of well defined steps that can be divided into two phases. The first phase involves maturation of germline stem cells (GSCs) into egg chambers from the ovary germarium (Gigliotti et al., 2000). Cell division of GSCs forms two daughter cells. One of these cells retains the GSC fate while the other becomes a cytoblast which will ultimately undergo mitotic cell division to form a 16 cell egg chamber (Gilboa and Lehmann, 2004). The rate of cell division of GSC's is regulated by genes which control the G1/S phase transition (Hatfield et al., 2005). Down regulation of one of these genes, Dacapo, results in an increased rate of GSC cell division. Recently it has been found that clonal mutants of the *dicer-1* gene have a reduced rate of GSC cell division and increased Dacapo expression (Hatfield et al., 2005). Ultimately, it was demonstrated that Dacapo expression is down regulated by the miRNA pathway enabling GSC cells to pass the G1/S transition of the cell cycle. It was also shown that this pathway is specific to GSC and dcr-1 mutations do not affect somatic G1/S phase transitions.

The findings reported by Hatfield and colleagues (2005) support a role for dsRBPs and the RNAi pathway in egg chamber formation. Perhaps a role will also be established for *DIP1* in germ cell development. Current evidence, including observation of a sterility phenotype and altered ovary morphology in two independently derived strains supports this possibility. In order to demonstrate a role for the *DIP1* gene in the ovary development pathway, further investigation of the nature of sterility in these two strains is required. Ovaries from both strains have been described as abnormally small and delicate. However, a more careful analysis of the ovary phenotypes observed in these strains is needed in order to classify more specifically the stage or process of ovary development and/or germ cell division that is being affected. It may also be interesting to investigate male sterility in the GE77 and BG2658 lines.

The EY*4 *DIP1* deletion was identified as a suppressor of repeat induced gene silencing.

An assay for involvement of DIP1 in regulation of mini-white array gene expression identified EY*4 as a suppressor of repeat induced silencing (Figure 11). Mini-white array repeat induced gene silencing involves recognition of a dsRNA followed by a cascade of events leading to silencing of the homologous genome. Evidence from fission yeast (Volpe et al., 2002) and *Drosophila* (Pal-Bhadra et al., 2004) support a link between the dsRNAi pathway and establishment of silencing of the homologous gene. This link supports the model for facultative heterochromatin formation that suggests dsRNA is recognized by the RNAi pathway (Reviewed in Allshire, 2002,Bayne and Allshire, 2005,Wassenegger, 2005). Subsequently, components of the RNAi pathway facilitate chopping up of the dsRNA into siRNA and lead to labeling of homologous regions of the genome for heterochromatin formation. Ultimately, dsRNA expression and recognition by the RNAi pathway plays a role in setting up facultative heterochromatin mediated gene silencing in the repeat induced gene silencing paradigm. The observed interaction between the EY*4 deletion and mini-white gene expression would appear to suggest a functional role for *DIP1* in repeat induced silencing. However, before any solid conclusions can be drawn the effects of other *DIP1* alleles on mini-white gene expression

must be investigated. In addition, measurements for a precise excision of the EY2625 P-element must be made as a negative control.

A complicating factor to consider is the preliminary observation that GE89 does not alter silencing in the repeat induced gene silencing paradigm. It would be expected that a deletion more extensive than the EY*4 line would exhibit a similar, if not more severe, interaction. However, an initial measurement of GE89 with the BX1 mini-white array was quantified as having an OD 480nm absorbance of 0.13. This measurement is not significantly different than the mean value for the BX1 array in a wild type background (0.073) and is significantly lower than the mean comparative result for EY*4;BX1/BX1 (0.7247). As only one measurement has been made for GE89;BX1/BX1 no statistical conclusions can be made however, this result can not be ignored in a discussion of a possible role for *DIP1* in the mechanism of repeat induced silencing. One possible explanation for this discrepancy in results is that, the interaction between EY*4 and repeat induced silencing is not due to an isoform specific loss of DIP1 expression. Instead, the results found with EY*4 may reflect missregulated expression of the DIP1 isoform not affected by the deletion.

To test the hypothesis that suppression of variegation in the repeat induced gene silencing paradigm by EY*4 is the result of missexpression of the DIP1a isoform, other isoform specific modifications of DIP1 gene expression should be looked at in the same system. To date the interaction between GE77 and the repeat induced gene silencing paradigm has not been investigated. This is due in part to the homozygous sterile phenotype of this line which complicates the crossing scheme required to place both the GE77 deletion and the mini-white arrays together. The GE77 deletion, like the EY*4 deletion, also leaves the coding region for the DIP1a isoform intact. Therefore, it may be expected that GE77 would also have an effect on repeat induced silencing. However, it is important to consider that the GE77 deletion, unlike EY*4, is also missing a significant portion of the 5' regulatory region. It may also be of interest to investigate the effect of overexpression of DIP1 isoform specific transgenes by the UAS-GAL4 system on repeat induced gene silencing.

The GE89 deletion of the *DIP1* gene appears to be a suppressor of PEV.

An assay looking at the impact of alleles of the *DIP1* gene and PEV identified GE89 as a suppressor of variegation (Figure 14). This result supports our hypothesis that DIP1 is involved in epigenetic regulation of gene expression. It also correlates well with a report that identified an interaction between Su(var)3-9, an established suppressor of PEV, and DIP1 in a yeast two-hybrid screen (Krauss et al., 2000,Krauss et al., 2001).

PEV in the X-inversion white gene silencing paradigm ($In(1)w^{m4}$) involves a mechanism of heterochromatin formation that differs from that described above for repeat induced silencing. In this paradigm, the white gene is moved next to a region of constitutive heterochromatin by a chromosomal inversion (Schotta et al., 2003). Silencing of genes bordering on heterochromatic regions has been proposed to occur by a method of 'spreading' (Richards and Elgin, 2002). It is important to note that, in this case heterochromatin formation does not appear to require a dsRNA intermediate or the involvement of the RNAi pathway.

The results of the PEV assay were a bit surprising in that EY*4, a deletion found to suppress repeat induced silencing, did not show a suppression of PEV phenotype. As discussed above it appears that not all isoforms of DIP1 are affected by the EY*4 deletion. Therefore, it is possible that DIP1 protein expression is maintained in EY*4 to a level sufficient to support formation of constitutive heterochromatin.

Another surprising result from the PEV assay is the finding that pigment expression in the GE8 precise excision was significantly higher than the $In(1)w^{m4}$ background level of expression. Although the measured levels of expression did not reach the levels found with the GE89 or Su(var)3-9 lines, it is of some concern that any alteration in eye pigment expression was detected at all. It is possible that this change arose from an interaction with something in the background of the Korean line. To test for this possibility it may be useful to look at another precise excision line derived from a different Korean P-element line.

Although both the repeat induced gene silencing and PEV paradigms have been utilized to identify modifiers of gene silencing, the mechanism for establishment of silencing in these two paradigms is different. In the case of repeat induced silencing recognition of dsRNA and targeting of homologous sequences is important. Where as, in the case of PEV, silencing occurs simply because of the location in the genome. These intrinsic differences may lead to conflicting findings when using both of these paradigms to identify modifiers of gene silencing. It is possible that a component of the silencing pathway that plays a role in recognition of dsRNA or targeting of the homologous gene sequences would alter silencing in the repeat induced gene silencing assay. However, no effect may be seen with the same component in the PEV assay. Perhaps such an occurrence can account for the different results obtained with the EY*4 allele in these two paradigms.

P-element insertion line GE50031 disrupts appendage formation.

Drosophila development results in the formation of adult structures in a well specified manner. Therefore, observations of structures differing from the expected form are of interest. Often, understanding the cellular and genetic alterations underlying these mutant phenotypes offers some explanation of the mechanisms involved in proper development. Thus, it was intriguing to observe disrupted leg formation in a noticeable number of flies from a P-element insertion strain, GE50031, with an insertion point in the 5' end of the *DIP1* gene (Figure 10). It was also noted that, complete removal of one copy of *DIP1,* by using a deficiency chromosome (Df(1)LB6), in combination with the P-element insertion showed an even higher frequency of disrupted leg phenotypes. In addition, precise excision of the GE50031 P-element reduced the frequency of observed leg phenotypes to less than 1% (Table 2). Taken together these observations suggest that the presence of the GE50031 P-element and, thus disrupted *DIP1* expression, may be the underlying cause of the observed leg phenotypes.

Evidence gathered by other researchers may also indicate a role for DIP1 in appendage development. Duplications of antenna and mouth structures as well as loss of arista were observed in adult flies when DIP1 was overexpressed in eye-antenal imaginal

discs (DeSousa et al., 2003). Investigation of the gene expression patterns underlying these phenotypes in the 3rd instar larval eye-antennal imaginal disc showed a duplication of the *distalless (dll)* expression pattern, loss of *spalt major (salm)* expression in the antennal portion of the eye disc and expansion of the *homothorax (hth)* expression region (DeSousa et al., 2003). Overexpression of DIP1 has a wide variety of developmental consequences. Thus, it is unlikely that DIP1 plays a specific instructive role in development. Instead, De Sousa and colleagues (2003) propose a role for DIP1 in epigenetic regulation of gene expression.

Formation of adult appendages in *Drosophila* arises from groups of cells termed imaginal discs. Cells in these domains are programmed in embryogenesis to take on specific cell fates upon adult appendage formation. It may by that DIP1 plays a role in establishing and or maintaining the specific patterns of gene expression responsible for proper appendage formation. Thus, the altered appendage phenotypes observed in flies with disrupted DIP1 expression patterns may occur as a consequence of missregulated establishment and/or maintenance of instructive gene patterns.

In considering a role for *DIP1* in the context of leg duplication formation it is important to note that there are still some questions as to whether the observed phenotypes are in fact due to a disruption of the *DIP1* gene. Firstly, it must be established whether or not *DIP1* expression is disrupted in the GE50031 insertion line. Also, the frequency of observed leg phenotypes must be established in several control stains, including a wild type strain and the Df(1)LB6 line, to further strengthen these results.

Future experiments will add to our understanding of the function of the *DIP1* gene.

Characterization of the *DIP1* gene thus far has suggested a possible functional role for this gene in epigenetic regulation of gene expression (DeSousa et al., 2003). The findings reported here also support this hypothesis. However, additional experimentation is required to draw further conclusions.

Generation of a complete null mutation of the DIP1 gene.

The first goal of further analysis of the *DIP1* gene may be to generate a completely null allele. Analysis of the function of DIP1 has been facilitated by the establishment of several deletions of the 5' end of this gene. However, in order to develop a more complete understanding of the function of the *DIP1* gene a fly strain that does not express any DIP1 protein must be generated.

P-element imprecise excision has been partially successful in disrupting the *DIP1* gene. Additional P-element excision screens will eventually yield a complete deletion of the *DIP1* gene. Alternatively, an RNAi approach to removal of gene expression may be used. In this method, transgenic constructs expressing dsRNA homologous to the target gene would be stably incorporated into the *Drosophila* genome. dsRNA expression is recognized by the PTGS pathway and ultimately represses expression of the homologous gene. Lee and Carthew (, 2003) have described an efficient RNAi vector that has previously been used successfully by another member of our lab (B. K. Dey) to knock out *disco* gene expression.

Does DIP1 act as a suppressor of silencing and PEV in other paradigms?

Firstly, analysis of the impact of the *DIP1* alleles and the silencing paradigms must be completed. To date, the EY*4 allele of *DIP1* has been shown to act as a suppressor of repeat induced silencing. Completion of this analysis including testing of both the GE89 and GE77 alleles in this paradigm will help develop our understanding of a potential role for *DIP1* in repeat induced gene silencing. Testing of precise excisions of both the EY2625 and GE50031 P-elements is also necessary. As well, a potential interaction between GE89 and position effect variegation ($In(1)w^{m4}$) was identified. Analysis with the GE77 allele in this paradigm must be completed.

In addition, it may be of interest in to investigate other PEV paradigms. Genetic analysis of established PEV gene *Su(var)3-9* was conducted with two other inversions: $In(2LR)bw^{V32g}$ and $In(1)sc^{8}$ (Tschiersch et al., 1994). $In(2LR)bw^{V32g}$ is an inversion of the second chromosome that relocates the brown eye pigment gene into an area of heterochromatin. Flies from this strain have brown eyes flecked with spots of red. The

effect of silencing on this element can also be quantified in the same manner as was done for $In(1)w^{m4}$. Investigation with the $In(2LR)bw^{V32g}$ strain offers some advantages to the $In(1)w^{m4}$ inversion. $In(2LR)bw^{V32g}$ is an inversion of the 2nd chromosome. So far the effects of the *DIP1* alleles on PEV have been looked at only as heterozygotes as both the inversion and the *DIP1* gene are on the X-chromosome. Utilization of the $In(2LR)bw^{V32g}$ strain available from the Bloomington stock centre would enable investigation of the *DIP1* alleles as homozygotes. Another strain to consider, $In(1)sc^{8}$, is an inversion of the X-chromosome that affects the expression of the *scute* gene. In this case, the effects of modulators of gene silencing can be measured by enumeration of the number of scutellar bristles expressed per fly. This method may be of interest as it is quantified in a different manner from the other paradigms previously discussed. However, like $In(1)w^{m4}$ this is also an inversion of the X-chromosome and thus measurements can only be made with *DIP1* in a heterozygous combination.

Recently, Pal-Bhadra and colleagues (2004) identified components of the RNAi machinery as also having an effect on silencing. This group looked at the effects of RNAi mutants on repeat induced silencing as well as PEV of P-elements inserted into pericentric heterochromatin and the 4th chromosome. It may also be of interest to look at the effects of the *DIP1* alleles on these silencing paradigms.

Is DIP1 associated with heterochromatin in vivo?

An abstract submitted to a regional *Drosophila* meeting (Krauss et al., 2000) indicated that DIP1 (aka Klett) binds distinct chromosomal bands. In order to further investigate a functional association of DIP1 with heterochromatin a ChIP assay may be useful. A method for this procedure was reviewed by Das and colleagues (Das et al., 2004). Chromatin immunoprecipitation (ChIP) involves crosslinking of chromatin with associated proteins *in vivo*. Following sonication to break the chromatin into pieces, immunoprecipitation using an antibody to the protein of interest is conducted to isolate chromatin pieces to which it is crosslinked. Subsequent PCR reactions are done to determine whether the isolated chromatin corresponds to regions of DNA suspected to be a target for the protein of interest. This technique may be useful to identify if DIP1 is

associated with specific heterochromatic sequences. However, before undertaking this experiment a more thorough evaluation of potential target DNA sequences should be conducted. Alternatively, the identification of the other proteins also associated with the immunoprecipitated chromatin may also be of interest. A procedure for acetone precipitation recovery of proteins has been described (Kuo and Allis, 1999). Western analysis using antibodies specific to known components of the heterochromatin remodeling complex such as Su(var)3-9 may identify if DIP1 is directly involved in this complex.

Is DIP1 a component of the RNAi pathway?

The evidence gathered to date supports the hypothesis that DIP1 plays a role in gene silencing. However, it is unknown in what capacity DIP1 fulfills this role. One possibility is that DIP1 is involved in the RNAi pathway. In order to further explore this hypothesis, the effect of disrupted DIP1 expression on RNAi mediated silencing may be investigated. Another member of our lab, Bijan Dey, has established a transgenic fly strain that down regulates *disco* gene expression via the RNAi pathway under the control of the UAS-Gal4 system. Under normal circumstances overexpression of *disco* by GMR-Gal4 causes a rough eye phenotype. Bijan has shown that simultaneous expression of the *disco*-RNAi element completely rescues the GMR-Gal4-UAS-*disco* rough eye phenotype. We hypothesize that, if DIP1 plays a role in the RNAi pathway, rescue of the GMR-Gal4-UAS-*disco* rough eye phenotype by expression of the *disco*-RNAi element will be incomplete or in some way disrupted in a DIP1 deletion background. An initial experiment was done looking at the effect of the EY*4 deletion on *disco*-RNAi. While no affect was found in this case it will be interesting to look for effects with the other available DIP1 alleles.

Do disruptions of DIP1 expression alter the patterns of expression of heterochromatin markers?

It has been shown previously that loss of biochemical markers of heterochromatin is associated with disruptions of the RNAi pathway (Pal-Bhadra et al., 2004,Volpe et al., 2002). An investigation of the effect of *DIP1* deletions on the expression patterns of heterochromatin markers such as HP1, H3K9Me and Su(var)3-9 will also be of interest.

REFERENCES

Allshire R. Molecular biology. RNAi and heterochromatin--a hushed-up affair. Science 2002; (297): 1818-1819.

Bayne E H, Allshire R C. RNA-directed transcriptional gene silencing in mammals. Trends Genet 2005; (21): 370-373.

Bellen H J, Levis R W, Liao G, He Y, Carlson J W, Tsang G, Evans-Holm M, Hiesinger P R, Schulze K L, Rubin G M, Hoskins R A, Spradling A C. The BDGP gene disruption project: single transposon insertions associated with 40% of Drosophila genes. Genetics 2004; (167): 761-781.

Bernstein E, Caudy A A, Hammond S M, Hannon G J. Role for a bidentate ribonuclease in the initiation step of RNA interference. Nature 2001; (409): 363-366.

Bondos S E, Catanese D J, Jr., Tan X X, Bicknell A, Li L, Matthews K S. Hox transcription factor ultrabithorax Ib physically and genetically interacts with disconnected interacting protein 1, a double-stranded RNA-binding protein. J Biol Chem 2004; (279): 26433-26444.

Bonin C P, Mann R S. A piggyBac transposon gene trap for the analysis of gene expression and function in Drosophila. Genetics 2004; (167): 1801-1811.

Campos A R, Lee K J, Steller H. Establishment of neuronal connectivity during development of the Drosophila larval visual system. J Neurobiol 1995; (28): 313-329.

Caudy A A, Hannon G J. Induction and biochemical purification of RNA-induced silencing complex from Drosophila S2 cells. Methods Mol Biol 2004; (265): 59-72.

Czermin B, Schotta G, Hulsmann B B, Brehm A, Becker P B, Reuter G, Imhof A. Physical and functional association of SU(VAR)3-9 and HDAC1 in Drosophila. EMBO Rep 2001; (2): 915-919.

Das P M, Ramachandran K, vanWert J, Singal R. Chromatin immunoprecipitation assay. Biotechniques 2004; (37): 961-969.

DeSousa D, Mukhopadhyay M, Pelka P, Zhao X, Dey B K, Robert V, Pelisson A, Bucheton A, Campos A R. A novel double-stranded RNA-binding protein, disco interacting protein 1 (DIP1), contributes to cell fate decisions during Drosophila development. J Biol Chem 2003; (278): 38040-38050.

Dillon N. Heterochromatin structure and function. Biol Cell 2004; (96): 631-637.

Dorer D R, Henikoff S. Expansions of transgene repeats cause heterochromatin formation and gene silencing in Drosophila. Cell 1994; (77): 993-1002.

Dorer D R, Henikoff S. Transgene repeat arrays interact with distant heterochromatin and cause silencing in cis and trans. Genetics 1997; (147): 1181-1190.

Doyle M, Jantsch M F. New and old roles of the double-stranded RNA-binding domain. J Struct Biol 2002; (140): 147-153.

Elgin S C, Grewal S I. Heterochromatin: silence is golden. Curr Biol 2003; (13): R895-R898.

Engels W R, Johnson-Schlitz D M, Eggleston W B, Sved J. High-frequency P element loss in Drosophila is homolog dependent. Cell 1990; (62): 515-525.

Filipowicz W. RNAi: the nuts and bolts of the RISC machine. Cell 2005; (122): 17-20.

Gigliotti S, Rotoli D, Manzi A, Graziani F, Malva C. Female sterile mutations and egg chamber development in Drosophila melanogaster. Int J Dev Biol 2000; (44): 581-589.

Gilboa L, Lehmann R. How different is Venus from Mars? The genetics of germ-line stem cells in Drosophila females and males. Development 2004; (131): 4895-4905.

Gloor G B, Preston C R, Johnson-Schlitz D M, Nassif N A, Phillis R W, Benz W K, Robertson H M. Engels W R. Type I repressors of P element mobility. Genetics 1993; (135): 81-95.

Grewal S I, Elgin S C. Heterochromatin: new possibilities for the inheritance of structure. Curr Opin Genet Dev 2002; (12): 178-187.

Grewal S I, Moazed D. Heterochromatin and epigenetic control of gene expression. Science 2003; (301): 798-802.

Grewal S I, Rice J C. Regulation of heterochromatin by histone methylation and small RNAs. Curr Opin Cell Biol 2004; (16): 230-238.

Hacker U, Nystedt S, Barmchi M P, Horn C, Wimmer E A. piggyBac-based insertional mutagenesis in the presence of stably integrated P elements in Drosophila. Proc Natl Acad Sci U S A 2003; (100): 7720-7725.

Hannon G J. RNA interference. Nature 2002; (418): 244-251.

Hatfield S D, Shcherbata H R, Fischer K A, Nakahara K, Carthew R W, Ruohola-Baker H. Stem cell division is regulated by the microRNA pathway. Nature 2005; (435): 974-978.

Henikoff S, Matzke M A. Exploring and explaining epigenetic effects. Trends Genet 1997; (13): 293-295.

Istrail S, Davidson E H. Logic functions of the genomic cis-regulatory code. Proc Natl Acad Sci U S A 2005; (102): 4954-4959.

Knight S W, Bass B L. A role for the RNase III enzyme DCR-1 in RNA interference and germ line development in Caenorhabditis elegans. Science 2001; (293): 2269-2271.

Kozak M. Interpreting cDNA sequences: some insights from studies on translation. Mamm Genome 1996; (7): 563-574.

Krauss V, O'Grady M, Hoffmann J, Schotta G, Fischer A, Kuhfittig S, Dorn R, Grigliatti T, Reuter G. KLETT, a *Drosophila* Chromatin Protein with dsRNA Binding Motifs interacts with the heterochromatin-associated SU(VAR)3-9 Protein. European Drosophila Conference . 2001. Abstract

Krauss V, O'Grady M, Kuhfittig S, Dorn R, Sass H, Grigliatti T, Reuter G. KLETT, a Novel *Drosophila* Protein with dsRNA Binding Motives is a SU(VAR)3-9-interacting Chromatin Component. RDM 2000 . Abstract

Kuo M H, Allis C D. In vivo cross-linking and immunoprecipitation for studying dynamic Proteir:DNA associations in a chromatin environment. Methods 1999; (19): 425-433.

Kurkulos M, Weinberg J M, Roy D, Mount S M. P element-mediated in vivo deletion analysis of white-apricot: deletions between direct repeats are strongly favored. Genetics 1994; (136): 1001-1011.

Lee Y S, Carthew R W. Making a better RNAi vector for Drosophila: use of intron spacers. Methods 2003; (30): 322-329.

Levine M, Davidson E H. Gene regulatory networks for development. Proc Natl Acad Sci U S A 2005; (102): 4936-4942.

Liao G C, Rehm E J, Rubin G M. Insertion site preferences of the P transposable element in Drosophila melanogaster. Proc Natl Acad Sci U S A 2000; (97): 3347-3351.

Ma J L, Kim E M, Haber J E, Lee S E. Yeast Mre11 and Rad1 proteins define a Ku-independent mechanism to repair double-strand breaks lacking overlapping end sequences. Mol Cell Biol 2003; (23): 8820-8828.

Mathieu O, Bender J. RNA-directed DNA methylation. J Cell Sci 2004; (117): 4881-4888.

McVey M, Radut D, Sekelsky J J. End-joining repair of double-strand breaks in Drosophila melanogaster is largely DNA ligase IV independent. Genetics 2004; (168): 2067-2076.

Michiels F, Gasch A, Kaltschmidt B, Renkawitz-Pohl R. A 14 bp promoter element directs the testis specificity of the Drosophila beta 2 tubulin gene. EMBO J 1989; (8): 1559-1565.

Motamedi M R, Verdel A, Colmenares S U, Gerber S A, Gygi S P, Moazed D. Two RNAi complexes, RITS and RDRC, physically interact and localize to noncoding centromeric RNAs. Cell 2004; (119): 789-802.

Nadershahi A, Fahrenkrug S C, Ellis L B. Comparison of computational methods for identifying translation initiation sites in EST data. BMC Bioinformatics 2004; (5): 14.

Nakayama J, Rice J C, Strahl B D, Allis C D, Grewal S I. Role of histone H3 lysine 9 methylation in epigenetic control of heterochromatin assembly. Science 2001; (292): 110-113.

Nassif N, Penney J, Pal S, Engels W R, Gloor G B. Efficient copying of nonhomologous sequences from ectopic sites via P-element-induced gap repair. Mol Cell Biol 1994; (14): 1613-1625.

Nicholson R H, Nicholson A W. Molecular characterization of a mouse cDNA encoding Dicer, a ribonuclease III ortholog involved in RNA interference. Mamm Genome 2002; (13): 67-73.

Nigg E A. Nucleocytoplasmic transport: signals, mechanisms and regulation. Nature 1997; (386): 779-787.

Pal-Bhadra M, Leibovitch B A, Gandhi S G, Rao M, Bhadra U, Birchler J A, Elgin S C. Heterochromatic silencing and HP1 localization in Drosophila are dependent on the RNAi machinery. Science 2004; (303): 669-672.

Pelka P. Molecular and Biochemical Characterization of DISCO Interacting Protein 1. 2000. McMaster. Master's Thesis.

Richards E J, Elgin S C. Epigenetic codes for heterochromatin formation and silencing: rounding up the usual suspects. Cell 2002; (108): 489-500.

Rivas F V, Tolia N H, Song J J, Aragon J P, Liu J, Hannon G J, Joshua-Tor L. Purified Argonaute2 and an siRNA form recombinant human RISC. Nat Struct Mol Biol 2005; (12): 340-349.

Sagai T, Hosoya M, Mizushina Y, Tamura M, Shiroishi T. Elimination of a long-range cis-regulatory module causes complete loss of limb-specific Shh expression and truncation of the mouse limb. Development 2005; (132): 797-803.

Saunders L R, Barber G N. The dsRNA binding protein family: critical roles, diverse cellular functions. FASEB J 2003; (17): 961-983.

Schotta G, Ebert A, Dorn R, Reuter G. Position-effect variegation and the genetic dissection of chromatin regulation in Drosophila. Semin Cell Dev Biol 2003; (14): 67-75.

Schotta G, Ebert A., Krauss V, Fischer A, Hoffmann J, Rea S, Jenuwein T, Dorn R, Reuter G. Central role of Drosophila SU(VAR)3-9 in histone H3-K9 methylation and heterochromatic gene silencing. EMBO J 2002; (21): 1121-1131.

Spradling A C, Stern D, Beaton A, Rhem E J, Laverty T, Mozden N, Misra S, Rubin G M. The Berkeley Drosophila Genome Project gene disruption project: Single P-element insertions mutating 25% of vital Drosophila genes. Genetics 1999; (153): 135-177.

St Johnston D, Brown N H, Gall J G, Jantsch M. A conserved double-stranded RNA-binding domain. Proc Natl Acad Sci U S A 1992; (89): 10979-10983.

Steller H, Fischbach K F, Rubin G M. Disconnected: a locus required for neuronal pathway formation in the visual system of Drosophila. Cell 1987; (50): 1139-1153.

Tower J, Karpen G H, Craig N, Spradling A C. Preferential transposition of Drosophila P elements to nearby chromosomal sites. Genetics 1993; (133): 347-359.

Tschiersch B, Hofmann A, Krauss V, Dorn R, Korge G, Reuter G. The protein encoded by the Drosophila position-effect variegation suppressor gene Su(var)3-9 combines domains of antagonistic regulators of homeotic gene complexes. EMBO J 1994; (13): 3822-3831.

Verdel A, Jia S, Gerber S, Sugiyama T, Gygi S, Grewal S I, Moazed D. RNAi-mediated targeting of heterochromatin by the RITS complex. Science 2004; (303): 672-676.

Volpe T A, Kidner C, Hall I M, Teng G, Grewal S I, Martienssen R A. Regulation of heterochromatic silencing and histone H3 lysine-9 methylation by RNAi. Science 2002; (297): 1833-1837.

Wallrath L L, Elgin S C. Position effect variegation in Drosophila is associated with an altered chromatin structure. Genes Dev 1995; (9): 1263-1277.

Wassenegger M. The role of the RNAi machinery in heterochromatin formation. Cell 2005; (122): 13-16.

Appendix A: Primer information

Location *(relative to 5' end of DIP1)*	Number	Description	Sequence
-2910	ML13632	Forward 1.6Kb 5' of BG2658	gaaaatcacgtaccacaattgtatcc
-1585	ML13334	Forward 5' of BG2658 insertion	caaattcaaactggcacatgtgcg
-641	ML11487	Forward	tcccactatctaagtaacagg
-111	ML11486	Reverse	caaagtgatggaaagacggc
-70	ML1751 (ML3556)	Forward	ctatggccagtgtgaaatgtctataatatatt
+41	ML13630	Reverse	gtcacagaaagaatcgtactgcactg
+41	ML1750	Forward	cagtgcagtacgattctttctgtgac
+902	ML13631	Reverse	ctgtttgcagagaggttcgag
+1415	AB28563	Forward Exon 1 5' of 2nd ATG	gcaaacgcagaattccaatgcca
+1778	AB28565 (ML3555)	Reverse	cttaccagacgagatcttgcgctt
+1906	AB28564	Reverse	cataggaattttagatcttaaactcgc
+2671	ML9008	Forward Intron 2	cagctcagacttcatgtccctag
+2811	ML9006	Reverse Intron 2	ctaaaggacagcactgctcccag
+3183	ML9004	Forward 5' of dsRBD1	gtattacttagtttccctcgcactgc
+3637	ML9007	Reverse 3' of dsRBD1	cgcgaacagcttgtagatggcaaac
+4187	ML9005	Reverse 3' of dsRBD2	gttgcgcaattgacgtcagggtc

Appendix B: Breakpoint sequence analysis

>EYstar4 (primer ML3556)
TAATACTAAAAACGATTTTCGAAATATGTGAAAAATATCGATATATTTACATATATTTTG
ACATCCCTACTTAAGTTTTTTACTTCAGTGCATGATGAAATAACAAAATAAAATTATTAT
AAATAAAATAAAAATAAATAAAATTTATAAAATTATAAACCACTGGACCAGTCCGCTGCA
AGTGATTTTGTCTAGGGTAGCCTGGCGAGCCAGGCGGAACCCGTTGCCTTCGCTAACTAA
TCGACTAATGAAACTCTTTCGCAAACGCAGAATCCCAATGCCACCGTCAAGCCTTTGATC
CAAATGCCGTTGCAGGCCGCCAATGTCCAGGAGCAGCAGTCTTCTCCGGTGGCTTTATAT
CCGACATCGGCCTCCCCGGTGGCTGTTCAATCGCCACAGGACGCATTTTTGGCTGTTCAG
TCGCCAGGGGCTCCTGCCCCCGTTCAACTGGCCAACTCGTCCGACCAGCAGAATAATCCG
GATGCGGACGCCATTGCCTCCAAACTGCCCATGCCAGTTATCATCAAGGAGGAGCCGATC
TCTGTCAACGATCAACCGTCCGTCGACAATATAGAGGACAATACCAGTGCCAGTACCAGT
GCCAGCGGCATCCGGGGGCAAGATCCCATTTAAAAAAATCTTCCAAAAGCGCAAGAAGTCG
TCTGGTAAGCGACGAAACCTTTGGTGATCAGATTTCCCAGAATTTTCACACGCTCACACA
AAGCACTAGGTTTCTTATGGAAGGGCAGACCGGAAATTACTTACAGTTGTGTTGCGAGTT
TAAGATCTATTTTCTTTTGGGGNNN

>EYstar4 (primer AB28564)
ACACAACTGTAACGTAATTTCCGGTCTGCCCTTCCaTAAGAAACCTAGTGCTTTGTGTGAG
CGTGTGAAAATTCCTGGGAAATCTGATCACCAAAGGTTTCCTCGCTTACCAGACGACTTCT
TGCGCTTTTGGAAGATTTTTTTAAATGGGATCTTGCCCCCGATGCCGCTGGCACTGGTAC
TGGCACTGGTATTGTCCTCTATATTGTCGACGGACGGTTCATCGTTGACAGAGATCGGCT
CCTCCTTGATGATTAACTGGCATGGGCAGTTTGGAGGCAATGGCGTCCGCATCCGGATTAT
TCTGCTGGTCGGACGAGTTGGCCAGTTGAACGGGGGCAGGAGCCCCTGGCGACTGAACAG
CCAAAAATGCGTCCTGTGGCGATTGAACAGCCACCGGGGAGGCCGATGTCGGATATAAAG
CCACCGGAGAAGACTGCTGCTCCTGGACATTGGCGGCCTGCAACGGCATTTGGATCAAAG
GCTTGACGGTGGCATTGGGATTCTGCGTTTGCGAAAGAGTTTCATTAGTCGATTAGTTAG
CGAAGGCAACGGGTTCCGCCTGGCTCGCCAGGCTACCCTAGACAAAATCACTTGCAGCGG
ACTGGTCCAGTGGTTTATAATTTTATAAATTTTATTTATTTTTATTTTATTTATAATAAT
TTTATTTTGTTATTTCATCATGCACTGAAGTAAAAAACTTAAGTAGGGATGTCAAAATAT
ATGTAAATATATCGATATTTTTCACATATTTCGAAAATCGTTTTTAGTATTAAATATATT
ATAGACATTTCACACTGGCCCATAGAANNNNN

>GE89 (primer ML11487)
TACTTACCtTACTTTGAGCaTTAGTATTTTTTTAATATATGCATAATATGAAAAACACAC
CTATTAATCCCAATGTAGATAGTTAATTCAGTTGATTTGGTGTTCATTTTTACAAAGTCG
CATACTTTCCTATTGCTGTAGTTGAGGAAACGCAAAACTTTTGTTAACACAGTGTGAAAA
CATTTCCTGTTTTTTTGTTGACGTTATAGATTTTGCCCACGCTGCAGACAGGCAAATTGTG
TTTGCAAGTCATGAAAAGTCATGCGCTTATGGTTCGAGTTCTATACTATTTTCTTAATAC
ATTTGAATGTCAGTCAGTCAAACAAAAATGTAGGGAATTACCATGCACACAATTTAACAG
CTATAATATTCTCGCGATATACAGAAGTACTGTTTCAATTCTAAATTTTCGCAATAACTT
TTAAGCACTTCCAAAGAGCATCGTCGTGCTATTTTTAGCATGCTTTTAATTATTTCACAA
TAAAATCTTTGGTCTGCTCTTTTTTTTCCGCCGTCTTTCCATCACTTTGCTTATATTACT
ATGGCCAGTGTGAAATGTCTATAATATATTTAATACTAAAAACGATTTTCGAAATATGTC
NAAAATATCGATATATTTACATATATTTTGACATCCCTACTTAAGTTTTTTACTTCAGTG
CATGATGAAATAAATGTTAAATAAAAAATTCCTATGTTTTATAGTTTTATTGGTCCATTT
TTTTTATNATATCCATTAGGTATTTAATTTTGAACAATTCAAAACATGTTTCACATTTATN
CCTTCACANGTTTCAAAAGTGTAGATTAAAACCCNTACTTAGGCCGAAATNCTTTTTCTT
TTAATATGTTAATTACGGCATACNCTTGGTGGGATANCCTTTGTTANCNANCCNAGNCCT
TACCCNCAGGCGGCATGGTGNCCACTNAGGTCCNTGGCACCGCTTTGGGGGATTNNCNCC
AGCATCTGCCACTTGNAAANNTNACCNANGNCGCGNCAATNTTTGNCCNNTNGTTAATNC
CCCCCNGGGTT

>GE89 (primer ML9006)
GgaAAgCTTAAGCTAAAAAAGAAAGGACAAACATATAAAGACATTCAAAAAACCATACTA
AACGTAAAACCACAGATATAGAGGATCGACGCATAGATAGTTCGTTAAAGCAAAGTCTAT
TCTTTTGCATACTCTAGGGACATGAAGTCTGAGCTGAACTTGGGAATCAGTGACGTTGCA
ATTCGGAGACGACCTACTTAATCAAAATTTAAGTGCGAAGAGCCCACGAAAGGTGCCCCTA
CTTAGCCAAAGGCATATTCAGACAAGGATAAACTTCGCTATGGGCTAGTTTTTTTTACAA
TGGTATGAGTCCATAAAATATGATTTTTGGTATTATAGACCAAAAGCGCATATGTAAATA
TTCTTAGTGATGTCTTACTGTCATATTCTGAATATAATATGCCCTTAAAATGGTCATTCC
AAAAGGATAATAAATCCGAAACGTAGAAGCAAATCGGCTAGGTTCACCCAAAATAGAATAG
ATGCCGAGGACAGCACCATCTTCCGATTTAAACTCGATTGAAACCCTGTGGGGGGACATT
AAACAATATGTGTCAAAGAACTGCCCGACGCCTAAGGCTCAGATTTGACAAGTTGTGCAG
GATGCATGGTCGAAATTCCCCCCAAGCGTTGCCAGGACCTAGTGGACACCATGCCGCATG
GGTGTAAGGCTGTGCTAGCTAACAAAGGCTATCCACCAAGTGTTATGCCGTAATTAACAT
ATTAAAAGAAAAAGAATTTCTGCCTATTATGTTGTTTTAATCTACACTTTTGAAACTATT
GAAGGANAAATGTGAACATGGTTTTGATTGTTNAAAATAAATNCCTAATGATATATAAAA
AAANGGCCANTAAACTATAAACNTNGGATTTTTTATTNAANNTTATTTCTNCNNCAGNGA
NNAAAAANTNANTNNGGTGNAAANNTNNNNAAATTNCNNNTTTTNNNNTTTNNNAANCNT
TNNNNNTAAATNNTANNCCTTNCCNTGCNNNNNANNANNAN

>GE77 (primer ML13631)
CtAAtTNAatTctAATAGAaTTTTCTCCGATATGCAAAAATAGAGTAAAATAATTGACTA
TTGACCTATACGTTTCACAATTCTGTCTATTTTAGCATGAAACAATAGTTATGGGGATCC
TTCGGTCATCGGCTGAGTTCATGGTCGCCGGCTCGTTTCGGGCACTTTCGGTGGAGTGAA
TGGGCATCAATAACTTTATATTGTTTCGAGAAATGCGGAAATATTTATTAGTTAGTATTA
GGATTCGTTAAAAAGTATGTAACAGGCAGAAGGAAGCGTTTCAGACTATATAAAGTATAT
GTATATAATAAACTTTTTTGGTAATTGATTAAATTAAAAAATATATATTTTTCTTTTTAT
AATCTTTATTTGATTAGTTTTTACCAGAGGTCAGTATTCTTTCGGCTCAGCAAACCTTTT
TCGGAGGATTAACATAATCCTTTTAAGTTCTACTTAGCTTTATATTTCAAGCTTATCGGA
TCATTAGGCTAGTTACCGTTAAGCGGTTGGTGTCTTAGGAGAATGTTATTTATGAAGCTT
CTGAAGAGTGAAGCTTTCCAAAAGATCGGCTTTAGCTTTTTATATGATGAGAGAATATGT
CACTTCCCCACCTTTTAGATATTAGCTTGTCATCAAGCGATTATTTCTGGATACAATTGT
GGTACNGGAATTTTCANNNNNNNNNNANN

>GE77 (primer ML13632)
AAGtAAtAATCGCTTGNGACAAGCTAATATCTAAAAGGTGGGGAAGTGACATATTCTCTC
ATCATATAAAAAGCTAAAGCCGATCTTTTGGAAAGCTTCACTCTTCAGAAGCTTCATAAA
TAACATTCTCCTAAGACACCAACCGCTTAACGGTAACTAGCCTAATGATCCGATAAGCTT
GAAATATAAAGCTAAGTAGAACTTAAAAGGATTATGTTAATCCTCCGAAAAAGGTTTGCT
GAGCCGAAAGAATACTGACCTCTGGTAAAAACTAATCAAATAAAGATTATAAAAAGAAAA
ATATATATTTTTTAATTTAATCAATTACCAAAAAAGTTTATTATATACATATACTTTATA
TAGTCTGAAACGCTTCCTTCTGCCTGTTACATACTTTTTAACGAATCCTAATACTAACTA
ATAAATATTTCCGCATTTCTCGAAACAATATAAAGTTATTGATGCCCATTCACTCCACCG
AAAGTGCCCGAAACGAGCCGGCGACCATGAACTCAGCCGATGACCGAAGGATCCCCATAA
CTATTGTTTCATGCTAAAATAGACAGAATTGTGAAACGTATAGGTCAATAGTCAATTATT
TTACTCTATTTTTGCATATCGGAGAAAATTCTATTAGAATTAGAATTAGATTTTCTCGAA
CCTCTCTGNCAAACAGAANNNNNNNNNNN

>GE8 (primer ML3556)
TAATACTAAAAACGATTTTCGAAATATGTGAAAAATATCGATATATTTACATATATTTTG
ACATCCCTACTTAAGTTTTTTACTTCAGTGCAGTACGATTCTTTCTGTGACCTGAGCAGT
GAAAAATTAAATTACAAAAGCGAAAAAGCGAATTACAAAAGTGAAAAATTAAATTACAAA
AAAAATCAAGATGAAGCGAAATCGTCGTGCATTTGCTGGAAACAACAAGCCATTTGTCTT
TGGAGGCATTTACGTAAGAATCTTAATTTTTTTTGCAAGTGTGTGCAGGAGTGTGAGTTA
AGAATTCCCTGTGACGTCACGAAGATATGTATTCCGAGTGAAAATGCATCACGAAAACAA
AAACCATTGTTGGAATCATCCATATTTGATTTGTGAAATAACAAAGTTTTCGTTTTTATT
TCTATAATTTGCAGCGCACAAAGTGAAAGTGTTCATTCACAATTCACCACAATTGTGAAC
TCATTTGCAATAGCCACTAAAAGCGGGTTAATCGAAAGTGCAGACCGTTGTCCGAATTCC
ACCAGCATTCACAATGCACCCCCCAGACATCCACCACCTTCCCCTCTCCCCTTACATTCG
TAACCCACCCATTTGCATTGCACTCATTCCACTCCGTTCGTGCTTTCGATCAACTAGATA
TGGGCCAGCACTGCTATAGTTTCACGCTGGACTTGCGGNTATCGCTAACTTTTATGGCTA
CTGAAATGCATTCACCCGAAACTGTACTAAATTATTAGTTTTGGGTCAGATAGCATGCCA
TTCNCTCACCGAAGTGCCGAACGAGCCGNGACATGACTCAGCCGTGACCGAGGACCCATA
CTTTGTTCATGCTAATAGAAGATTGGGAACGTTAGNCATAGTCATTTTTACTTTTTTTGC
ANTCGGGAANANANTNTTTAAATANATTNATTTTNNGACCTTTTGAACNGAAACTTNNGAAN
GTACCCCCTGGCTGATTTTTGTACCGNCTTN

>GE50031 (P-primer towards AB28564)
atTnnGCtTcagTGCAGTACGATTCTTTCTGTGACCTGAgCAGTGAAAAATTAAATTACA
AAAGCGAAAAAGCGAATTACAAAAGTGAAAAATTAAATTACAAAAAAAATCAAGATGAAG
CGAAATCGTCGTGCATTTGCTGGAAACAACAAGCCATTTGTCTTTGGAGGCATTTACGTA
AGAATCTTAATTTTTTTTGCAAGTGTGTGCAGGAGTGTGAGTTAAGAATTCCCTGTGACG
TCACGAAGATATGTATTCCGAGTGAAAATGCATCACGAAAACAAAAACCATTGTTGGAAT
CATCCATATTTGATTTGTGAAATAACAAAGTTTTCGTTTTTATTTCTATAATTTGCAGCG
CACAAAGTGAAAGTGTTCATTCACAATTCACCACAATTGTGAACTCATTTGCAATAGCCA
CTAAAAGCGGGTTAATCGAAAGTGCAGACCGTTGTCCGAATTCCACCAGCATTCACAATG
CACCCCCCAGACATCCACCACCTTCCCCTCTCCCCTTACATTCGTAACCCACCCATTTGC
ATTGCACTCATTCCACTCCGTTCGTGCTTTCGATCAACTAGATATGGCCAGCACTGCTAT
AGTTTCACGCTGGACTTGCGGTTATCGCTAACTTTTATGGCTACTGAAAATGCATTCACC
CGAAACTGTAACTAAAATTATTAGTTTTGGGTCAGATAGCAATGCCCATTCACTCCACCG
AAAGTGCCCGAAACGAGCCGGCGACCATGAACTCAGCCGATGACCGAAGGATCCCCATAA
CTATTGTTTCATGCTAAAATAGACAGAATTGTGAAACGTATAGGTCAATAGTCAATTATT
TACTCTATTTTGCTATCGGAGAAATTTCTTTAGATTAGATTAGATTTCTCGACCTCTCTG
CAACAGATCATAGCGAAAGTACTCNCNTGAGCTGATTATTGTACCGACTTGGGTTTATGC
CNTTGATAAAGCTGGTACCTATGGAGCACTGNTTCTGTACTNCTCTGTCGAGTCTGCTGN
CATACGAATCNNCCTGANTGTCGTGNNACTCTCGGCTGNCAGTGCTGTGTCGCTGTTATA
CNCNCCGCGCGATGCNTGGTCTGCNGCTTGNCTGCNCTANNTNTGACGACGACTCTNNNT
NNGNTC

Appendix C: GE50031, GAL4 results (Crosses done at 29°C)

GE50031/Y X GE50031/GE50031

GE50031/GE50031	GE50031/Y
19	208

GE50031/FM7 X GE50031/Dp(1:Y)

GE50031/GE50031	GE50031/FM7	GE50031/Dp(1:Y)	FM7/Dp(1:Y)
0	47	23	17

GE50031/Dp(1:Y) X Act5CGal4/CyO

GE/+;Act/+	+/Dp;Act/+	GE/+;CyO/+	Dp/+;CyO/+
33	18	20	18

GE50031/GE50031 X DppGal4/TM6B,Tb,Hu

GE/+;DppGal4/+	GE/Y;DppGal4/+	GE/+;TM6B,Tb,Hu/+	GE/Y;TM6B,Tb,Hu/+
45	16	19	3

GE50031/Y X dllGal4/CyO

GE/+;dllGal4/+	Y/+;dllGal4/+	GE/+;CyO/+	Y/+;CyO/+
163	113	151	130